MATHEMATICAL MODEL FOR CHOLERA DYNAMICS WITH VACCINATION AND TEMPERATURE DEPENDENT PARAMETER

Kennedy Owade Jackob

A Research Thesis Submitted in Partial Fulfillment of the Requirements for the Award of the Degree of Doctor of Philosophy in Applied Mathematics of Masinde Muliro University of Science and Technology

November, 2024

DECLARATION

This thesis is my original work prepared with no other than the indicated sources and support and has not been presented elsewhere for award of degree or any other award.

Signature..... Date .....

Kennedy Owade Jackob

SEA/H/01-53211/2018

CERTIFICATION

The undersigned certify that they have read and hereby recommend for acceptance of Masinde Muliro University of Science and Technology a thesis entitled;
"Mathematical Model for Cholera Dynamics with Vaccination and Temperature Dependent Parameter"

Signature..... Date .....

Dr. Akinyi Colleta

Department of Mathematics,

Masinde Muliro University of Science and Technology, Kakamega - Kenya.

Signature..... Date .....

Dr. Frankline Tireito

Department of Mathematics,

Masinde Muliro University of Science and Technology, Kakamega - Kenya..

COPYRIGHT

DEDICATION

To my dad Hezron Saggia

ACKNOWLEDGEMENTS

I would like to express my sincere gratitude to my supervisors Dr. Colleta Akinyi and Dr. Frankline Tireito who encouraged me to attempt this study where I have profited tremendeously in disease modelling. Through you I have achieved this and may God grant you many more years. I would also wish to thank the entire Masinde Muliro University of Science and Technology Mathematics Department led by Chair, Prof. Achiles Nyongesa Simiyu, for both material and moral support during the study period. Special thanks to Prof. George Lawi and Dr. Charles Muriuki Wachira who kept on encouraging and informing me that one day it shall be over. To my parents who instilled in me the importance of education and gave me the foundation from which to soar, I say thank you so much for always encouraging me to keep on pressing. Without forgetting my fiancee Mary Juma who has always been their for me and contributed tremendeously when I was in need financially, may God bless you. Finally to the Almighty God, thank you for revealing to me these mathematical insights.

ABSTRACT

Cholera is an acute intestinal infection caused by ingesting *Vibrio cholerae*. It is severely contagious acute bacterial infection which is caused by colonization and multiplication of *Vibrio cholerae* inside the small intestine. When ingested, the binding sub units of the enterotoxin combine extraordinarily rapidly to the molecules in the cell wall of the intestine. The binding then becomes irreversible within minutes since they become incorporated into the cell membrane and eventually results into modification of the binding protein which leads to rapid excretion of electrolytes into the small intestine. Health providers have put several control measures into place such as provision of clean water, improved food safety, good sanitation and more so availability and access of vaccine which is administered to stimulate the immune system to produce antibodies for protection. Despite the use of the vaccine, cholera epidemics are still very frequent. Most of the cholera vaccine mathematical models so far done are between-host models. Mathematical modelling of the dynamics of *Vibrio cholerae* within the human host has largely remained unexplored yet it is the interaction between the bacteria and the cells of the small intestine that play a major role in the dynamics of the cholera disease. In this research, a within-host cholera mathematical model has been developed using a system of ODEs incorporating vaccine efficacy. The solutions of the model have been shown to be well-posed. The vaccine R_{0V} has been done using the next generation matrix approach. Analysis of the model shows that IFE point is both locally and globally asymptotically stable when $R_{0V} < 1$ and IE point is locally asymptotically stable when $R_{0V} > 1$. Further analysis shows the existence of backward bifurcation. To highlight the relevance of vaccine efficacy, numerical simulation of the model with respect to vaccination is carried out and shows that when the vaccine efficacy γ is high, there will be lower infection rate of cells. Due to the existence of backward bifurcation in the within-host cholera model with vaccination, there is shedding out $Vibrio\ cholerae$ to the environment whose multiplication is affected by changes in temperatures, it is for this reason that a between-host mathematical cholera model with temperature dependent parameter is formulated to investigate the effect of temperature change on the dynamics of cholera disease. Analysis of the model shows that DFE point is both locally and globally asymptotically stable when $R_0 < 1$ and EE point is locally asymptotically stable when $R_0 > 1$. Sensitivity analysis shows that increasing the temperature of the environment would help reduce the infection rate of the pathogen thus reduce the reproduction number R_0. Numerical simulation of the model has been carried out with respect to temperature change and the analysis shows that cholera pathogens can multiply and spread faster under temperatures of 23^0C but between the temperature range of $23^0C < T \leq 43^0C$ their multiplication and spread is lowered. Finally this research adopts the use of Caputo fractional order time derivative to analyse the dynamics of between-host cholera model and the results compared to that obtained from the ordinary order derivatives and it shows that the fractional order simulated results gave a better understanding of how temperature of the environment is key to the control of the disease.

TABLE OF CONTENTS

List of Tables

List of Figures

List of Abbreviations and Acronyms

DFE	-Disease Free Equilibrium
EE	-Endemic Equilibrium
IFE	-Infection Free Equilibrium
IE	- Infection Equilibrium
CTX	- Cholera Toxin
WHO	- World Health Organization
MATLAB	- Mathematics Laboratory
DFE	- Disease Free Equilibrium
EE	- Endemic Equilibrium

CHAPTER ONE

INTRODUCTION

1.1 Background of the Study

Cholera is an acute diarrhoeal infection caused by ingestion of food or water contaminated with the bacterium *Vibrio cholerae*. Cholera remains a global threat to public health and an indicator of inequity and lack of social development.

1.1.1 Clinical Manifestation of *Vibrio cholerae*

Cholera is an acute illness caused by an enterotoxin elaborated by *Vibrio cholerae* that when ingested colonizes the small intestine. After 24hrs to 48hrs incubation period, cholera begins with sudden onset of painless water diarrhea that mainly quickly become voluminous and often followed shortly by vomiting. In severe cases, stool volume can exceed 250 ml/kg in the first 24hrs. Fever is usually absent, muscle cramps due to electrolyte disturbances are common. The stool has a characteristic appearance; a non-bilious, grey, slightly cloudy fluid with flecks of mucus, no blood, and somewhat sweet and in-offensive odor. It has been called 'rice-water' stool because of its resemblance to the water in which rice has been washed. Clinical symptoms, parallel volume contraction shows losses of $(3-5)$ percent of normal body weight. If fluids and electrolytes are not replaced, hypovolemic shock and death will occur [16].

1.1.2 Pathogenesis of *Vibrio cholerae*

For *Vibrio cholerae* to colonize the small intestine and produce cholera toxin (CTX), it must colonize, control and traverse several hostile environments, the first of this is the milieu of the stomach. *Vibrio cholerae* lacks genetically con-

trolled mechanism of acid resistance, rather, it relies on a large inoculum size to allow some organisms to elude the bacterial effects of gastric acidity. If successful, it must next traverse the mucus layer of the upper small bowel[16].

Several properties of the organism enhance its ability to accomplish this feat, including its motility, chemotaxis and production of protease originally named cholera lectin which is able to cleave mucin and fibronectin as well as the A sub-unit of CTX. The protease also serve to detach vibrios found in the small bowel surface, thus facilitating their spread within the intestine and excretion in the stool. The activated A sub-unit irreversibly transfers $ADP - rybosylation$ to its specific target protein, the binding regulatory component of *adenylate cyclase* in intestinal epithelial cells. When ADP-ribosylated, the G protein regulates the catalytic sub-unit, the result is the intracellular accumulation of high levels of cyclic AMP from ATP. In turn, cyclic AMP inhibits the absorptive transport system in vilius cells and activates the excretory chloride transport system in crypt cells and these leads to the accumulation of sodium chloride in the intestinal lumen. Since water moves positively to maintain osmolality, isotonic fluid accumulates in the lumen. Then when the volume of the fluids exceeds the capacity of the rest of the gut to re-absorb it, watery diarrhea results. Unless the wasted fluid and electrolytes are adequately replaced, shock follows which could result to death[16].

According to the studies of natural infection, the human body has T-lymphocytes cell and B-lymphocytes cell which produce antibodies that attack the pathogens thereby providing protection. However, in a situation of excess consumption of bacteria the body may not defend itself, as a result there is need for vaccination [8].

The World Health Organization (WHO) recommends the use of oral cholera vaccines, *Dukoral* and *Shanchol* for those at high risk [39]. When these vaccines are administered, the cholera strain within the vaccine produce an incomplete, non-toxic version of the toxin, the body then responds to the safe version of cholera and creates an immunity to the infection through production of antibodies (T-lymphocytes cells and B-lymphocytes).

Despite the availability and access of cholera vaccines, there is still high burden of cholera in endemic areas [39][40]. Experimental studies have shown that the vaccines have efficacy protection of about 66 percent with a period of protection of 3-5 years [39]. This research is focused on formulating within-host cholera vaccination model to investigate the impact of cholera vaccine on the dynamics of the in-host cholera infection in the small intestine.

A study [28] has shown that the dynamics of epidemic models are determined by the disease's basic reproduction number, R_0. Epidemiologists generally know that if $R_0 < 1$, the disease can be eliminated from the community and the epidemic occurs when $R_0 > 1$ [9]. Despite $R_0 < 1$, studies [3],[2] and [17] have established that infectious diseases can still persist.

With continuous persistence of cholera outbreak between human population, studies have shown that cholera incidence have been predominant when there is always interchange of seasons (dry to wet seasons and vice versa)[15] and [20]. The quality and quantity of drinking, irrigation, environmental and recreational waters can be associated with changes in environmental conditions that includes weather or

climate related variables. Floods may cause the overflow of waste-water treatment plants, failure of septic systems, or combined sewer overflows, which could contaminate nearby water surfaces or wells. Furthermore, there is increasing concern about pathogens in storm water runoff [15][40]. Also maintaining sanitary water conditions is an issue during drought conditions, when contaminants may become concentrated in available water. Additionally, the likelihood of multiple uses in a water body may increase i.e cleaning, bathing, and drinking during droughts and consequently enhance the risk of contamination of water and exposure to cholera disease [18][46].

A study by Christaki *et al* [6] the impact of climate change on cholera. The study finding shows that water ecosystems can be rather sensitive to evolving or sudden changes in weather parameters and the changes can result in alterations in the natural habitat of pathogens, vectors, and human hosts, as well as in the transmission dynamics and geographic distribution of infectious agents. The study further shows that the interaction between climate change and infectious disease is rather complicated and not deeply understood. It is for this reason that in this study a between host mathematical cholera model with temperature dependent parameter is formulated to investigate the effect of temperature change on the dynamics of cholera disease.

Finally, the between-host cholera model with temperature dependent parameter developed is expressed in Caputo fractional order derivative and analysed to predict the dynamics of cholera disease with changes in temperature. This is because mathematical models developed in fractional order are useful than the ordinary order model as it can be used in predicting outbreaks of infectious diseases [4].

Fractional order derivative models are also suitable in data fitting, useful in giving information about the memory that can describe the model in real cases and has hereditary property [4].

Fractional-order Caputo derivative has also gained a lot interest in solving problems in science. For instance [36] Caputo fractional derivative has been used to analyze the tuberculosis infection a case study Pakistan and the results shows that the Caputo model provides a better approximation to the reported infected cases [36]. Motivated by the this discussion, this study adopted the use of Caputo fractional order time derivative to analyse and predict the dynamics of cholera disease with temperature dependent parameter.

1.2 Statement of the Problem

Cholera is a bacterial infection of the small intestine of humans. Cholera control measures such as improved food safety, use of safe drinking water and proper sanitation have been put in place to the public. Vaccines against cholera infection are also available in the public but the disease has remained persistently endemic with regular outbreaks. It is not clear if the vaccine-in-host interaction is adequate to sustain prolonged protection against cholera disease. However, most between host cholera models have shown stable endemic equilibrium in cholera endemic areas. The study focused on developing a within-host cholera model with vaccination to investigate the impact of cholera vaccine on the dynamics of the in-host infection of cholera disease. With persistence of cholera outbreak, studies have shown that cholera incidence have been predominant when there is always interchange of seasons (dry to wet seasons and vice versa) which makes it difficult to understand the dynamics of cholera disease outbreak, this research therefore focused on developing a between host mathematical cholera model with temperature dependent

parameter to investigate the effect of change in temperature on the dynamics of cholera disease.

1.3 Objectives of the Study

1.3.1 General Objective

The main objective of this study was to develop and analyze a mathematical cholera model with vaccination and temperature dependent parameter using system of ordinary differential equations.

1.3.2 Specific Objective

The specific objectives of this study are:

(i)To develop and analyze a deterministic mathematical model of within-host cholera dynamics with vaccination.

(ii) To develop and analyze a deterministic between-host cholera mathematical model with temperature dependent parameter

(iii) To analyze the dynamics of Caputo-fractional order time derivative between-host cholera model with temperature dependent parameter.

1.4 Justification of the Study

Cholera outbreak has attracted global attention due to continued number of cases of cholera mortalities [42][40]. Much is being done about controlling the infection in cholera prone areas, such as provision of improved food safety and use of cholera vaccine yet cholera disease is still persistently endemic with regular epidemic outbreak. Existing within-host cholera models formulated investigated the interaction between the intestinal walls and the vibrio. Guided by the fact that despite the availability of the vaccine, there is still frequent cholera outbreaks. This study

focused on developing a within-host cholera model with vaccination to investigate the impact of cholera vaccine on the dynamics of the in-host infection cholera disease. According to the study [1], temperature drives the disease transmission through various traits of the pathogen population such as reproduction, development and lifespan. Theoretical work has also established that most physiological and life history traits respond non linearly to temperature [1], as a result in this study, a between host cholera model is developed and analysed to investigate the effect of temperature change on the dynamics of cholera disease.

1.5 Significance of the Study

This study will guide policy makers and health practitioners in making decisions such as vaccinating individuals against cholera in cholera endemic areas before an outbreak. Also, temperature being a determining factor in the multiplication of *Vibrio cholerae*, this study is relevant in that there is need to heat/warm food before consumption. The formulation and analysis of the model will also make contribution to the body of knowledge in Biomathematics (disease modelling).

CHAPTER TWO

LITERATURE REVIEW

2.1 Introduction

Cholera, an ancient disease, has been a major health threat to the third world countries. Several cholera outbreaks have been reported in recent years, for instance recently in Kenya in the year 2022, according to acting Director General for health in Kenya, Dr Patrick Amoth, the outbreak whose origin was traced to a wedding festival in Kiambu County was spread across Kiambu (31) cases, Nairobi (17) cases, Murang'a (1) case, Kajiado (2) cases, Nakuru (2) cases and Uasin Gishu (8) cases [19]. Also in Haiti between $2010-2012$ and in Zimbabwe between $2008-2009$ cholera outbreaks occurred with very high mortality rate. Cholera disease can be transmitted from the environment to individuals ingesting contaminated food and water, between individuals through direct and indirect contact with those infected e.g by shaking hands. This section therefore gives an overview of literature concerning within-host cholera models, between-host cholera models and fractional order derivative models.

2.2 Within-host and Between-host Cholera Models

Xueying Wang and Jin Wang [48] formulated a model linking within-host and between-host interaction is given as follows:

$$\begin{aligned}
\frac{dS}{dt} &= \mu N - \beta_H ZSI - \beta_L \frac{SB}{K+B} - \mu S + \sigma R \\
\frac{dI}{dt} &= \beta_H ZSI + \beta_L \frac{SB}{K+B} - (\gamma + \mu) I \\
\frac{dB}{dt} &= \gamma I - (\mu + \sigma) R
\end{aligned} \tag{2.1}$$

Z is the concentration of vibrios in humans, β_H is human transmission and β_L is the environment transmission. The formulation of the within-host dynamics given as follows:

$$\frac{dZ}{dt} = \frac{1}{\epsilon}uB + vZ - \rho Z \tag{2.2}$$

Where vZ is the intrinsic growth of human vibrios, μB is the rate at which the environmental vibrios are ingested in human body, ρZ is the rate at which human vibrios are removed due to shedding or death of vibrios and ϵ is the constant emphasizing time scale. The environmental factor linking within and between host is given as follows:

$$\frac{dB}{dt} = \epsilon(Z)I - \delta Z \tag{2.3}$$

$\epsilon(Z)$ is the shedding rate of the vibrio that depends on human vibrios, δ is the degradation rate of B (natural death and other forms of removal) and B is the concentration of the vibrio. Their results show that dynamics of the coupled system can be recovered by those of the slow and fast systems obtained by the fast-slow approximations. They suggested that incorporation of the immunological modelling principles with detailed pathogen - cell interactions into the model will enrich the within-host dynamics, and lead to potentially deeper understanding of the disease mechanism. The model assumes that the growth of human vibrios only depends on the environmental vibrios and the intrinsic dynamics of the human vibrios despite the within-host cholera dynamics may also connect to several epidemiological factors such as the disease prevalence.

Wang J and Modnak C [41] developed a between-host mathematical cholera model with controls given as follows:

$$\begin{aligned}
\frac{dS}{dt} &= \mu N - \beta_e S\frac{B}{k+B} - \beta_h SI - \mu S - v(t)S \\
\frac{dI}{dt} &= \beta_e S\frac{B}{k+B} - \beta_h SI - (\gamma+\mu)I - a(t)I \\
\frac{dB}{dt} &= \epsilon I - \delta B - w(t)B
\end{aligned} \tag{2.4}$$

μ denotes the natural human birth/death rate, ϵ is the rate of human contribution (e.g. shedding) to *Vibrio cholerae*, δ is the natural death rate of *Vibrio cholerae*, γ is the rate of recovery from cholera and β_e and β_h represent rates of ingesting vibrio from the contaminated water and through human-to-human interaction respectively. Vaccination is introduced to the susceptible population at a rate of $v(t)$, so that $v(t)S(t)$ individuals per time are removed from the susceptible class and added to the recovered class. Therapeutic treatment is applied to the infected people at a rate of $a(t)$, so that $a(t)I(t)$ individuals per time are removed from the infected class and added to the recovered class and water sanitation leads to the death of vibrios at a rate of $w(t)$. Their simulation results show that different controls (such as vaccination and treatment) closely interplay with each other. Further analysis shows that a combination of multiple intervention methods generally achieves better results than a single control such as vaccination only.

A multi-scale cholera model linking between-host and within-host dynamics was developed by Chayu Yang *et al* [7] to investigate the transmission dynamics of cholera disease. The model emphasized on the different levels of infection among human individuals in the within-host dynamics;

$$\begin{aligned}
\frac{dZ_i}{dt} &= C_i B - \sum\nolimits_i Z_i \\
\frac{dB}{dt} &= \alpha B(1-\frac{B}{K}) + \sum_{i=1}^{N} p_i \sum_i Z_i - \delta B
\end{aligned} \tag{2.5}$$

Where $i = 1, 2, ..., N$ The within-host dynamics is connected to the between-host dynamics through an environmental equation that characterizes the growth of the pathogen and its interaction with the hosts outside the human body.

Xueying Wang and Jin Wang [45] developed a within-host dynamics of cholera with bacterial-viral interaction given as follows:

$$\begin{aligned} \frac{dB}{dt} &= \Lambda - \alpha \frac{B}{K+B} V - \sigma_1 B \\ \frac{dZ}{dt} &= g(Z) + \theta_1 \alpha \frac{B}{K+B} V - \sigma_2 Z \\ \frac{dV}{dt} &= h(V) + \theta_2 \alpha \frac{B}{K+B} V - \sigma_3 V \end{aligned} \tag{2.6}$$

Where B represents environmental vibrios, Z human vibrios, V concentration of the virus (cholera toxin phage), α is the contact rate between the environmental vibrios and the virus and $g(Z)$ and $h(V)$ is the intrinsic growth rate of Z and V respectively. Their main focus is the interaction of environmental vibrios, human vibrios and the vibrios within the human host since such interaction is critical in shaping the evolution of the pathogen within human body and directly contributes to the epidemiology of cholera at the population level, since the human vibrios shed out of human body will remain highly infectious for a certain period of time and can be transmitted among human hosts. They established the basic reproduction number as a sharp threshold for disease dynamics such that when $R_0 < 1$, the highly infectious vibrios will not grow within the human host and the environmental vibrios ingested into human body will not cause cholera infection and when $R_0 > 1$, the human vibrios will grow and persist, leading to human cholera.

Conrad Ratchford and JinWang [12] developed cholera within-host model for an average infected individual given as follows:

$$\begin{aligned} \frac{dZ}{dt} &= C_1BV - d_1MZ - \epsilon Z \\ \frac{dV}{dt} &= C_2BV - d_2MV - \tau V \\ \frac{dM}{dt} &= e_1MZ + e_2MV - pM \end{aligned} \tag{2.7}$$

which is the fast scale system where Z, V, and M represent the concentrations of human vibrios, pathogen and host immune cells, respectively. The dynamics of the environmental evolution of the vibrios is governed by the equation given as follows:

$$\frac{dB}{dt} = \epsilon(Z)I - \delta B$$

Is the low scale system, where $\epsilon(Z)$ is the host shedding rate that depends on the human vibrios. In their analysis, the within-host dynamical system proposed is expanded to include the influence of human virus (cholera toxin phage) and immune cell interaction with the infectious vibrios and they findings shows that the slow-scale and intermediate scale systems act predictably and the dynamics of the smaller of the two combined systems depends mostly on R_0. However, the study recommends a complete stability analysis of the equilibrium of the full system of particular interest and they suggest that numerical simulation using real world data should be done to shed more light onto the likelihood of various assumptions.

This study focused on developing a within-host cholera model with vaccination investigating the impact of vaccination on the dynamics of in-host infection of cholera disease.

2.3 Mathematical Models with Temperature Dependent Parameter

In this section, we take a look at the mathematical models that have incorporated the relationship between temperature and infectious diseases but the first step towards understanding the relationship between temperature and disease is to define "normal" body temperature, from where deviations can be measured. For instance, many attempts has been made to this end, including the 1868 seminal paper by Wunderlich [43], who is believed to be the first to establish a link between fever and clinical diagnosis. He was also the first to apply a thermometer experimentally to measure human body temperature. Using a large sample size, Wunderlich [43] concluded that the average axillary human body temperature is 37.0^0C, with the upper limit of normal defined as 38.0^0C. However, newer studies challenged Wunderlich's [43] "normothermia" [29]. Furthermore, research has shown that body temperature is a function of several variables such as age ,gender, time of the diurnal cycle and more so environmental temperature and state of health [26] and [27]. Below are some description of mathematical models that show the relationship between infectious diseases and temperature changes.

Md Arquam *et al* [30] developed an SIR model for Vector-Borne diseases integrating environmental temperature conditions given as follows:

$$\begin{aligned}
\frac{dS_{hk(t)}}{dt} &= -\beta_h(k)S_{hk}(t)I_{hk}(t) - \beta_{vh}b(T)S_{hk}(t)I_n(t) \\
\frac{dI_{hk(t)}}{dt} &= \beta_h(k)S_{hk}(t)I_{hk}(t) + \beta_{vh}b(T)S_{hk}(t)I_v(t) - \mu_h I_{hk}(t) \\
\frac{dR_{hk(t)}}{dt} &= \mu_h I_{hk}(t)
\end{aligned} \tag{2.8}$$

Where $b(T)$ is the bitting rate that is dependent on temperature. The study investigated the effect of temperature on spreading of vector-borne diseases. The study

concluded that favourable temperature increases the disease spreading from vector to host and by cascading effect to the host population. The study further shows that the threshold of spreading rate of the disease is proportional to the square of the biting rate $b(T)$ which is defined as the function of temperature. Simulations are performed using the SIR model using an homogeneous contact network and shows that temperature increases the critical threshold value of the spreading rate of the disease.

Eunice *et al*[14] developed a mathematical model of the impact of temperature variations and immigration on malaria prevalence in Nigeria. The study examines the population-level impact of temperature variability and immigration on malaria prevalence in Nigeria using a novel deterministic model. The model incorporates disease transmission by immigrants into the community. In the absence of immigration, the model is shown to exhibit the phenomenon of backward bifurcation. The disease-free equilibrium of the autonomous version of the model was found to be locally asymptotically stable in the absence of infective immigrants. However, the model exhibits an endemic equilibrium point when the immigration parameter is greater than zero. The endemic equilibrium point is seen to be globally asymptotically stable in the absence of disease-induced mortality. Numerical simulations of the model show that in Nigeria, malaria burden increases with increasing mean monthly temperature in the range of $(22 \text{ to } 28)^0C$.

Salisu M. and Danbaba [33] developed a mathematical modelling of the effect of temperature variability on malaria control strategies. The population of wholly susceptible humans is generated by birth at a constant rate. This population increases through the loss of vaccination-acquired immunity by wholly vaccinated

individuals and is decreased by vaccination. Proportion of these individuals acquire malaria infection following effective contact with infectious mosquitoes at a temperature dependent rate $\lambda H(T)$, given as follows:

$$\lambda H(T) = \frac{\beta_{VH} M_I(t)}{N_V(t)}(1 - \epsilon_B \alpha_B)\alpha_M(T)$$

In the study, a non-autonomous (temperature dependent) and autonomous (temperature independent) models for the transmission dynamics of malaria in a population are designed and analysed. The models are used to assess the impact of temperature changes on various control strategies. The autonomous model is shown to exhibit the phenomenon of backward bifurcation, where an asymptotically-stable disease-free equilibrium (DFE) co-exists with an asymptotically-stable endemic equilibrium when the associated reproduction number is less than unity. Sensitivity analysis using temperature data is used to assess the parameters that have the most influence on malaria transmission. The partial rank correlation coefficient for the use of larvicides is positively correlated with the vaccinated reproduction number when the temperature ranges between (15 to 20)^0C and (30 to 35^0C), thus within those temperature intervals, use of larvicides may impede effort aimed at reducing malaria infection.

Based on the above studies, this study focused on developing a between-host cholera model with temperature dependent parameter, the infection rate of the pathogen α_1 that is dependent on temperature is incorporated both on long and short cycle transmission roots to investigate the dynamics of cholera disease with change in temperature.

2.4 Fractional Order Derivatives Models

A study [21] developed a fractional order model for cholera disease transmission with control strategies given as follows:

$$\begin{aligned}
D_t^q S(t) &= \lambda^q - (1-\theta^q)\beta_h^q S(t)I(t) - \frac{(1-\omega_2^q)\beta_e^q S(t)B(t)}{K^q + B(t)} - (\mu^q + \theta^q)S(t) \\
D_t^q I(t) &= (1-\theta^q)\beta_h^q S(t)I(t) - \frac{(1-\omega_2^q)\beta_e^q S(t)B(t)}{K^q + B(t)} - (\mu^q + d^q + \omega_1^q \alpha^q)I(t) \\
D_t^q B(t) &= \delta^q I(t) - (\omega_2^q + \delta^q)B(t) \\
D_t^q R(t) &= \omega_1^q \alpha^q I(t) + \theta^q S(t) - \mu^q R(t)
\end{aligned} \tag{2.9}$$

The result of the study shows that at different values of order of derivative, the solution profile of the model attains its stability at the equilibrium point. The control measures investigated in this study were health education campaigns, hygiene practices and treatment of infected individuals.

Sani and Mohammed [35] developed a Caputo sense fractional order derivative model of cholera and analysed the dynamics of cholera disease with controls. The control measures studied includes treatment, hygiene consciousness and vaccine, the results were produced in graphs to show the dynamics of the susceptible, effects of vaccine on the susceptible and the rate of cholera infection. The result show that lower fractional order values in the range 0.25 to 0.5 gives lower values of susceptible and vaccinated individuals but gives higher number of infected individuals.

The findings of the study [35] further shows that the fractional order results gave a better and efficient, portray of the successful useable controls. However, this study did not consider the effect of environmental conditions such as temperature

on the transmission dynamics of the disease, as a result, this study adopts the use of Caputo fractional order time derivative to analyse the dynamics of between-host cholera model with temperature dependent parameter.

CHAPTER THREE

DYNAMICS OF WITHIN-HOST INFECTION CHOLERA MODEL WITH VACCINATION.

3.1 Introduction

In this chapter a within-host cholera model with vaccination is developed to investigate the impact of vaccination on the dynamics of in-host infection of cholera disease in the human small intestine. In section (3.2) the model is described and formulated, in section (3.3) positivity and boundedness of solutions of the model are investigated, in section (3.4) the basic reproduction number is determined, in section (3.5) stability analysis at the equilibrium points are analysed and in section (3.6) numerical simulation of the formulated model is done to investigate the impact of cholera vaccine on the dynamics of in-host infection of cholera disease.

3.2 Model Description and Formulation

Cholera infection involves the interaction between the vibrio V and the target cells B. The target cells B are recruited at a constant rate Λ and they die naturally at a rate μ_1. Multiplication of the vibrio within the small intestine is given by $\beta_V V$, the recruitment rate of the vibrio is given by $h_V Z$. The interaction of vibrio within the small intestine with the target cells B leads to the infection of target cells at the rate αBV, where α is the contact rate between the target cells and the vibrios in the small intestine that leads to production of infected cells Z. The infected cells die naturally at a rate μ_2, and they are shed out at a rate d. The saturation incidence rate is given by $\frac{\alpha BV}{1+\delta V}$ such that δ is the measure of saturation level of the vibrio. The natural clearance rate of the vibrio and shedding rate is given by σ and s, respectively. The vaccine whose efficacy is γ with proportion

of non-effectiveness of the vaccine given by $1-\gamma$ exposes an individual to a dose of live cholera bacteria, which causes the body to produce antibodies against the disease.

The system of ordinary differential equation governing the description previously is as follows:

$$\begin{aligned} \frac{dB}{dt} &= \Lambda - (1-\gamma)\frac{\alpha BV}{1+\delta V} - \mu_1 B \\ \frac{dZ}{dt} &= (1-\gamma)\frac{\alpha BV}{1+\delta V} - (d+\mu_2)Z \\ \frac{dV}{dt} &= h_V Z + \beta_V V - (\sigma + s)V \end{aligned} \tag{3.1}$$

3.2.1 Assumptions of the Model.

Target cells are recruited at a constant rate

3.3 Positivity and Boundedness of the Model.

Since model (3.1) describes human cells, it should be well posed. Thus in this section, positivity and boundedness solutions of model (3.1) are discussed. Positivity of solutions of the model (3.1) is determined using the following initial conditions (3.2):

$$B(0) = B_0 \geq 0, Z(0) = Z_0 \geq 0, V(0) = V_0 \geq 0. \tag{3.2}$$

3.3.1 Positivity of the Model

Proposition 3.3.1. *Solutions of model (3.1) with initial condition (3.2) are positive in the region defined as* $\mathbb{R}^3{}_+ = \{(B, Z, V) | B \geq 0, Z \geq 0, V \geq 0\}$.

Proof. Let $N = sup\{t > 0 | B > 0, Z > 0, V > 0\}$. For the first equation of model (3.1) given as follows:

$$\frac{dB}{dt} = \Lambda - (1-\gamma)\frac{\alpha BV}{1+\delta V} - \mu_1 B = \Lambda - (1-\gamma)\frac{\alpha V}{1+\delta V} + \mu_1)B \qquad (3.3)$$

From this the integrating factor is $e^{\int_0^t (1-\gamma)\frac{\alpha V(\tau)}{1+\delta V(\tau)}d\tau + \mu_1(t)}$

Multiplying (3.3) by the integrating factor yields;

$$\frac{dB(t)e^{\int_0^t (1-\gamma)\frac{\alpha V(\tau)}{1+\delta V(\tau)}d\tau + \mu_1(t)}}{dt} \geq \Lambda e^{\int_0^t (1-\gamma)\frac{\alpha V(\tau)}{1+\delta V(\tau)}d\tau + \mu_1(t)}$$

Solving the inequality yields $B(t)e^{\int_0^t (1-\gamma)\frac{\alpha V(\tau)}{1+\delta V(\tau)}d\tau + \mu_1(t)} - B(0) \geq \int_0^t \Lambda e^{\int_0^k (1-\gamma)\frac{\alpha V(\tau)}{1+\delta V(\tau)}d\tau + \mu_1(t)dt}$

Therefore $B(t)$ becomes;

$$B(t) \geq B(0)e^{-\int_0^t (1-\gamma)\frac{\alpha V(\tau)}{1+\delta V(\tau)}d\tau + \mu_1(t)} +$$
$$e^{-\int_0^t (1-\gamma)\frac{\alpha V(\tau)}{1+\delta V(\tau)}d\tau + \mu_1(t)} \times \int_0^t \Lambda e^{\int_0^k (1-\gamma)\frac{\alpha V(\tau)}{1+\delta V(\tau)}d\tau + \mu_1(k)dk} > 0$$

Thus $B(t) > 0$.

From the second equation of model (3.1) given as follows:

$$\frac{dZ}{dt} = (1-\gamma)\frac{\alpha BV}{1+\delta V} - (d+\mu_2)Z = (1-\gamma)\frac{\alpha BV}{1+\delta V} - (d+\mu_2)Z \qquad (3.4)$$

The integrating factor is $e^{\int_0^t (d+\mu_2)td\tau}$

Multiplying (3.4) by the integrating factor yields;

$$\frac{dZ(t)e^{\int_0^t (d+\mu_2)td\tau}}{dt} \geq (1-\gamma)\frac{\alpha BV}{1+\delta V}e^{\int_0^t (d+\mu_2)td\tau}$$

Solving the inequality yields $Z(t)e^{\int_0^t(d+\mu_2)td\tau)} - Z(0) \geq \int_0^t(1-\gamma)\frac{\alpha BV}{1+\delta V}e^{\int_0^k(d+\mu_2)t)d\tau}$

Therefore $Z(t)$ becomes;

$$Z(t) \geq Z(0)e^{-\int_0^t(d+\mu_2)td\tau} + e^{-\int_0^t(d+\mu_2)td\tau} \times \int_0^t(1-\gamma)\frac{\alpha BV}{1+\delta V}e^{\int_0^k(d+\mu_2)t)d\tau>0}$$

Thus $Z(t) > 0$.

In a similar manner to the third equation of model (3.1) as follows;

$$\frac{dV}{dt} = \beta_V V - (\sigma + s)V \tag{3.5}$$

From this the integrating factor is $e^{\int_0^t(\sigma+s)dt}$

Multiplying (3.5) by the integrating factor yields;

$$\frac{dV(t)e^{\int_0^t(\sigma+s)dt}}{dt} \geq (\beta_V V)e^{\int_0^t(\sigma+s)dt}$$

Solving the inequality yields as follows:

$$V(t)e^{\int_0^t(\sigma+s)dt} - V(0) \geq \int_0^t(\beta_V V)e^{\int_0^k(\sigma+s)dk} \tag{3.6}$$

Therefore $V(t)$ becomes $V(t) \geq V(0)e^{-\int_0^t(\sigma+s)dt} \times \int_0^t(\beta_V V)e^{\int_0^k(\sigma+s)dk} > 0$

Thus $V(t) > 0$.

Hence, all the solution of model (3.1) given initial conditions (3.2) at any time t are positive. Therefore, the population of target cells and infected cells in human will continue to grow positively.

□

3.3.2 Boundedness of the Model

Since the model formulated describes cells in a human being, the population of the target cells and the infected cells will always remain bounded as shown below.

Proposition 3.3.2. *Let $t_0 > 0$. If $B_0 > 0$, $Z_0 > 0$ and $V_0 > 0$ then $B(t)$, $Z(t)$ and $V(t)$ will each remain nonnegative and bounded in $\in \mathbb{R}^3$ for all $t \in [0, t_0]$.*

Proof. Let $N(t) = B(t) + Z(t)$, where N is the total number of cells and let $\mu = \mu_1 = \mu_2$. From the system of equation (3.1), we have

$$N'(t) \leq \Lambda - (\mu_2 Z) \leq \Lambda - \mu N(t)$$

$$N'(t) \leq \Lambda - \mu N(t)$$

Integrating both sides of $N'(t) \leq \Lambda - \mu N(t)$ yields;

$$\int N'(t)dt \leq \int (\Lambda - \mu N(t))dt =$$

$$N(t)e^{\mu t} \leq \int \frac{\Lambda}{\mu} e^{\mu t} dt$$

Integrating the right side of $N(t)e^{\mu t} \leq \int \frac{\Lambda}{\mu} e^{\mu t} dt$ with respect to (t) yields

$$N(t)e^{\mu t} \leq \frac{\Lambda}{\mu} e^{\mu t} + C$$

$$N(t) \leq \frac{\Lambda}{\mu} + Ce^{-\mu t}$$

$$\lim_{t\to\infty} N(t) \leq \frac{\Lambda}{\mu}$$

Hence $N(t)$ is bounded, since solutions of model (3.1) are positive and bounded for $t \geq 0$; therefore, model (3.1) is mathematically and epidemiologically meaningful and is sufficient to consider its solution in Φ. □

3.3.3 Existence of Infection Free Equilibrium (IFE) Points

These are steady state solutions in absence of cholera disease in the body; therefore, target cells are not infected. Stability analysis is carried out to predict the long term behaviour of the solutions of the model (3.1).

Proposition 3.3.3. *For the model (3.1) IFE point is given by* $IFE = (B_0, Z_0, V_0) = (\frac{\Lambda}{\mu_1}, 0, 0)$.

Proof. At IFE, $Z = 0$,$V = 0$. Therefore considering the first equation in system (3.1) and replacing $Z = 0$,$V = 0$ and equating its right hand side to 0 yields

$$\Lambda - \mu_1 B = 0$$

$$\Lambda = \mu_1 B$$

Making B the subject yield

$$B = \frac{\Lambda}{\mu_1} \tag{3.7}$$

Therefore the infection free equilibrium point of system (3.1) is $(\frac{\Lambda}{\mu_1}, 0, 0)$. This shows that the infected class is zero since there are no pathogens and the entire population of cells consists of target cells only and their growth is bounded by $\frac{\Lambda}{\mu_1}$. □

3.4 Basic Reproduction Number, R_0.

The basic reproduction number R_0 is the epidemiological measurement of the transmission potential of cholera disease in a given population of human cells. Hence, when vibrio enters into a population of target cells it will infect them.

Definition 3.4.1. *The reproduction number R_0 is defined as the average number of secondary infections produced by a unit infectious cholera pathogen over the course of its infectious period in uninfected target cell population [38].*

Lemma 3.4.1. *The vaccine reproduction number of model system (3.1) is given by;*

$$R_{0V} = \frac{h_V(1-\gamma)\alpha B}{(d+\mu_2)(\sigma+s-\beta_V)}$$

Proof. Using the method of next generation matrix approach given by [38] to determine the basic reproduction number R_0. Consider the matrix

$$M = FK^{-1}.$$

F is the jacobian of $\mathcal{F}$ which refers to the rate of new infection of cells and K is the Jacobian of $\mathcal{K}$ which refers to the rate of transfer of infected cells from one compartment to another. From model (3.1) the associated matrices are;

$$\mathcal{F} = \begin{pmatrix} \frac{(1-\gamma)\alpha BV}{1+\delta V} \\ 0 \end{pmatrix} \tag{3.8}$$

$$\mathcal{K} = \begin{pmatrix} (d+\mu_2)Z \\ -h_V Z + (\sigma+s-\beta_V)V \end{pmatrix} \tag{3.9}$$

The jacobian matrices of (3.8) and (3.9) are;

$$F = \begin{pmatrix} 0 & (1-\gamma)\alpha B \\ 0 & 0 \end{pmatrix} \tag{3.10}$$

$$K = \begin{pmatrix} d+\mu_2 & 0 \\ -h_V & (\sigma+s-\beta_V) \end{pmatrix} \tag{3.11}$$

The inverse of matrix K is;

$$K^{-1} = \begin{pmatrix} \frac{1}{(d+\mu_2)} & 0 \\ \frac{h_V}{(d+\mu_2)(\sigma+s-\beta_V)} & \frac{1}{(\sigma+s)-\beta_V} \end{pmatrix} \tag{3.12}$$

Therefore,

$$M = FK^{-1} = \begin{pmatrix} h_V \frac{(1-\gamma)\alpha B}{(d+\mu_2)(\sigma+s-\beta_V)} & \frac{(1-\gamma)\alpha B}{(\sigma+s-\beta_V)} \\ 0 & 0 \end{pmatrix} \tag{3.13}$$

The intervention strategy in this study is the vaccine efficacy; hence, the associated reproduction number is referred to as vaccine reproduction number denoted R_{0V}; it is the threshold quantity that predicts the spread of cholera disease in a given population of target cells in presence of vaccination. Therefore, the vaccine reproduction number $R_{0V} = \rho(FK^{-1})$ which is the spectral radius of the matrix FK^{-1} is;

$$R_{0V} = \frac{h_V(1-\gamma)\alpha B}{(d+\mu_2)(\sigma+s-\beta_V)} \tag{3.14}$$

The calculated R_{0V} depends on vaccine efficacy and when $R_{0V} < 1$ there will be elimination of infected cells due to the action of vaccine. The vaccine reproduction number, R_{0V} being the measure of severity of an epidemic, it determines whether or not cholera disease will invade target cell population.

Epidemiologically this implies that if $R_{0V} < 1$, cholera infection will die out and if $R_{0V} > 1$, cholera infection will persist in cell population. □

3.5 Stability Analysis

The stability at the IFE determines the short-term epidemics of the infection of cells, while its dynamics over a longer period of time is characterized by the global stability at the IFE. In this section, the analysis of local and global stability of IFE and local stability of IE is done.

3.5.1 Local Stability of the Infection Free Equilibrium (IFE)

Theorem 3.5.1. *For any time $t \geq 0$, the infection free equilibrium $IFE = (\frac{\Lambda}{\mu_1}, 0, 0)$ of model (3.1) is locally asymptotically stable whenever $R_{0V} < 1$ and unstable whenever $R_{0V} > 1$.*

Proof. The jacobian matrix of (3.1) is given as follows;

$$J = \begin{pmatrix} \frac{-(1-\gamma)\alpha V}{1+\delta V} - \mu_1 & 0 & \frac{-(1-\gamma)\alpha\Lambda}{\mu_1(1+\delta V)} \\ \frac{(1-\gamma)\alpha V}{1+\delta V} & -(d+\mu_2) & \frac{(1-\gamma)\alpha\Lambda}{\mu_1(1+\delta V)^2} \\ 0 & h_V & \beta_V - (\sigma+s) \end{pmatrix} \tag{3.15}$$

Evaluating the IFE points in the jacobian matrix (3.15) at $IFE = (\frac{\Lambda}{\mu}, 0, 0)$ yields;

$$J_{IFE} = \begin{pmatrix} -\mu_1 & 0 & \frac{-(1-\gamma)\alpha\Lambda}{\mu_1} \\ 0 & -(d+\mu_2) & \frac{(1-\gamma)\alpha\Lambda}{\mu_1} \\ 0 & h_V & \beta_V - (\sigma+s) \end{pmatrix} \tag{3.16}$$

The matrix (3.16) in terms of R_{0V} yields;

$$J_{IFE} = \begin{pmatrix} -\mu_1 & 0 & \frac{-(1-\gamma)\alpha\Lambda}{\mu_1} \\ 0 & -(d+\mu_2) & \frac{(1-\gamma)\alpha\Lambda}{\mu_1} \\ 0 & h_V & \beta_V - (\sigma+s) \end{pmatrix} \tag{3.17}$$

For asymptotic stability all the eigenvalues should be strictly negative. It can be seen clearly that $\lambda_1 = -\mu_1$

From (3.17) consider the matrix A

$$A = \begin{pmatrix} -(d+\mu_2) & \frac{(1-\gamma)\alpha\Lambda}{\mu_1} \\ h_V & \beta_V - (\sigma+s) \end{pmatrix}$$

The trace of A is $-(d+\mu_2)+[\beta_V-(\sigma+s)]$. The trace will be negative if $(\sigma+s) > \beta_V$ The determinant of A $= -(d+\mu_2)[\beta_V - (\sigma+s)] - [h_V(1-\gamma)\alpha B]$. This implies that the determinant $= -(d+\mu_2)[\beta_V - (\sigma+s)] - R_{0V}(d+\mu_2)[(\sigma+s) - \beta_V]$. This can be written as det (A) $= (d+\mu_2)[(\sigma+s) - \beta_V] - R_{0V}(d+\mu_2)[(\sigma+s) - \beta_V]$. When the determinant is simplified, it becomes det (A)$= (d+\mu_2)[(\sigma+s)-\beta_V][1-R_{0V}]$. Whenever $(\sigma+s) - \beta_V > 0$ and $R_{0V} < 1$, det> 0 .

This shows that IFE is locally asymptotically stable whenever $R_{0V} < 1$ otherwise unstable.

This implies that with small perturbation of IFE, the solution of model (3.1) will eventually converge to IFE whenever $R_{0V} < 1$.

Epidemiologically it implies that if a few infectious cholera pathogens are introduced into a population of target cells, the disease would die out when $R_{0V} < 1$, otherwise the cholera disease would spread into population of target cells. □

3.5.2 Global Stability of the Infection Free Equilibrium (IFE)

The global stability of the IFE of the model (3.1) is explored using Castilo-Chavez [11]. The model (3.1) is rewritten in the form;

$$\frac{dH(t)}{dt} = L(X(t), Z(t))$$
$$\frac{dZ(t)}{dt} = G(X(t), Z(t)), G(X(t), 0) = 0$$

Where $X(t) = B(t)$, $X(t) \in \mathbb{R}_+$ denotes the uninfected cells and $Z(t) \in \mathbb{R}_+$ denoting the number of infected cells . At IFE there are no cells infected which implies that $Z(t) = 0$ and $V(t) = 0$. Hence

$$IFE = (X^*, Z^*), X^* = (\frac{\Lambda}{\mu_1}, 0)$$

The conditions;

$$\frac{dX(t)}{dt} = H(X(t), 0), X^*$$
$$G(X(t), Z(t)) = MZ - \hat{G}(X(t), Z(t)), \hat{G}(X(t), Z(t)) \geq 0 \tag{3.18}$$

X^* is globally asymptotically stable, Where $M = D_Z G(X^*, 0)$ is a Metzler matrix (the off diagonal elements of (M) are non-negative). If model (3.1) satisfies the conditions above (3.18), then Theorem (3.5.2) holds.

Theorem 3.5.2. *The fixed point $IFE = (X^*, 0)$ is globally asymptotically stable equilibrium point of model (3.1) whenever the $R_{0V} < 1$ whenever conditions (3.19) are satisfied, otherwise unstable.*

Proof. From model (3.1), at DFE we obtain;

$$H(X(t), 0) = \begin{pmatrix} \Lambda - \mu_1 B \\ 0 \\ 0 \end{pmatrix} \tag{3.19}$$

And

$$G(X(t), Z(t)) = M(t)Z(t) - \hat{G}(X(t), Z(t))$$

Where

$$M = \begin{pmatrix} -(d+\mu_2) & \frac{(1-\gamma)\alpha\Lambda}{\mu_1} \\ 0 & \beta_V - (\sigma + s) \end{pmatrix} \tag{3.20}$$

And

$$\hat{G}(X(t), 0) = \begin{pmatrix} \hat{G}_1(X(t), Z(t)) \\ \hat{G}_2(X(t), Z(t)) \end{pmatrix} = \begin{pmatrix} 0 \\ 0 \end{pmatrix} \tag{3.21}$$

Since $\hat{G}(X(t), Z(t)) > 0$ and the conditions (3.19) are satisfied, IFE is globally asymptotically stable whenever $R_{0V} < 1$ otherwise unstable.

This implies that given a large perturbation of the IFE, the solutions of the model (3.1) will eventually converge to IFE whenever $R_{0V} < 1$.

Epidemiologically, this means that if large number of vibrios are introduced to a population of target cells, cholera disease would die off hence elimination of infection in cells since there are no secondary infection produced whenever $R_{0V} < 1$, otherwise cholera disease would persist. □

3.5.3 Local Stability of the Infection Equilibrium (IE) Point

Infection Equilibrium (IE) points is the state at which the disease persists in the cells. We investigate the local stability of infection equilibrium points at $E^*(B^*, Z^*, V^*)$.

Theorem 3.5.3. *The infection equilibrium point $E^*(B^*, Z^*, V^*)$ of system (3.1) is locally asymptotically stable whenever $R_{0V} > 1$, otherwise unstable.*

Proof. The infection equilibria $E^*(B^*, Z^*, V^*)$ of model (3.1) is obtained by equating model (3.1) to zero then solving.

$$\Lambda - (1-\gamma)\frac{\alpha BV}{1+\delta V} - \mu_1 B = 0$$

$$(1-\gamma)\frac{\alpha BV}{1+\delta V} - (d+\mu_2)Z = 0$$

$$h_V Z + \beta_V V - (\sigma + s)V = 0$$

The following equilibrium points are obtained by solving the above equations in *Theorem* 3.5.3 simultaneously:

$$\begin{aligned} B^* &= \frac{[(d+\mu_2)][(1+\delta V^*)]Z^*}{(1-\gamma)\alpha V^*} \\ V^* &= \frac{(\delta+s)-\beta_V}{h_V} Z^* \end{aligned} \tag{3.22}$$

Now, the jacobian matrix of (3.1) evaluated at E^* is given as follows:

$$J_{E^*} = \begin{pmatrix} \frac{-(1-\gamma)\alpha V^*}{1+\delta V^*} - \mu_1 & 0 & -[\frac{(1-\gamma)\alpha B^*}{(1+\delta V^*)}] \\ \frac{(1-\gamma)\alpha V^*}{1+\delta V^*} & -(d+\mu_2) & [\frac{(1-\gamma)\alpha B^*}{(1+\delta V^*)^2}] \\ 0 & h_V & \beta_V - \sigma + s) \end{pmatrix} \tag{3.23}$$

For the linearized system (3.1), the characteristic polynomial is expressed as follows:

$$\mid J - \lambda I \mid = 0 \tag{3.24}$$

When (3.23) is substituted into (3.24), it yields

$$\begin{vmatrix} \frac{-(1-\gamma)\alpha V^*}{1+\delta V^*} - \mu_1 - \lambda & 0 & -[\frac{(1-\gamma)\alpha B^*}{(1+\delta V^*)}] \\ \frac{(1-\gamma)\alpha V^*}{1+\delta V^*} & -(d+\mu_2) - \lambda & [\frac{(1-\gamma)\alpha B^*}{(1+\delta V^*)^2}] \\ 0 & h_V & \beta_V - (\sigma+s) - \lambda \end{vmatrix} = 0 \tag{3.25}$$

Solving (3.25) yields;

$$[-m-\mu_1-\lambda][-(d+\mu_2)-\lambda][n-\lambda]-[\frac{(1-\gamma)}{(1+\delta V^*)^2}\alpha B^*]h_V+[\frac{(1-\gamma)}{(1+\delta V^*)}\alpha B^*][m][n-\lambda]=0 \tag{3.26}$$

Let

$$m = [\frac{(1-\gamma)}{1+\delta V^*}\alpha V^*]$$

$$n = [\beta_V - (\sigma+s)]$$

$$V^* = \frac{(\delta+s)-\beta_V}{h_V}Z^*$$

$$c = [\frac{(1-\gamma)}{(1+\delta V^*)^2}\alpha B^*]h_V$$

$$z = [\frac{(1-\gamma)}{(1+\delta V^*)}\alpha B^*][\frac{(1-\gamma)}{(1+\delta V^*)}\alpha V^*]$$

Then equation (3.26) can be written as

$$[-m-\mu_1-\lambda][-(d+\mu_2)-\lambda][n-\lambda]+z[n-\lambda]-c=0 \tag{3.27}$$

Expanding equation (3.27) yields;

$$[\lambda^3-\lambda^2[(m-\mu_1)-(d+\mu_2)+n]+\lambda[[(m+\mu_1)(d+\mu_2)+(m-\mu_1)n]+(m+\mu_1)(d+\mu_2)+z]$$

-

$$n[(m+\mu-1)(d+\mu_2+z)]+c=0$$

Solving the above cubic equation yields;

$$\lambda_1 = -[n[(m+\mu-1)(d+\mu_2+z)]+c]$$

Implying that $\lambda^2+\lambda[(m+\mu_1)(d+\mu_2)+(m-\mu_1)n]+[(m+\mu_1)(d+\mu_2)+z]=0$ and

$$\begin{aligned}\lambda_{2,3} &= \frac{-[(m+\mu_1)(d+\mu_2)+(m-\mu_1)n]}{2} \\ &\pm\frac{\sqrt{[(m+\mu_1)(d+\mu_2)+(m-\mu_1)n]^2-4(m-\mu_1)(d+\mu_2)}}{2}\end{aligned} \tag{3.28}$$

Now the eigenvalues $\lambda_1 = -[n[(m+\mu-1)(d+\mu_2+z)]+c]$ and the second eigenvalue is as follows:

$$\begin{aligned}\lambda_2 &= \frac{-[(m+\mu_1)(d+\mu_2)+(m-\mu_1)n]}{2} \\ &-\frac{\sqrt{[(m+\mu_1)(d+\mu_2)+(m-\mu_1)n]^2-4[(m+\mu_1)(d+\mu_2)+z]}}{2}\end{aligned} \tag{3.29}$$

and the third eigenvalue is as follows:

$$\begin{aligned}\lambda_3 &= \frac{-[(m+\mu_1)(d+\mu_2)+(m-\mu_1)n]}{2} \\ &+\frac{\sqrt{[(m+\mu_1)(d+\mu_2)+(m-\mu_1)n]^2-4[(m+\mu_1)(d+\mu_2)+z]}}{2}\end{aligned} \tag{3.30}$$

If $4[(m+\mu_1)(d+\mu_2)+z] > [(m+\mu_1)(d+\mu_2)+(m-\mu_1)n]^2$, then the square root part of $\lambda_{2,3}$ yields an imaginary root hence a possibility of backward bifurcation [2] which is an indication of the oscillatory behaviour in cholera outbreaks; also, *Theorem* (3.5.3) implies that a small perturbation of IE, the solution of model (3.1), will always converge to IE whenever $R_{0V} > 1$. Since $\lambda_1 = [n[(m+\mu-1)(d+\mu_2+z)]+c]$ and $\lambda_{2,3} = \frac{-[(m+\mu_1)(d+\mu_2)+(m-\mu_1)n]\pm\sqrt{[(m+\mu_1)(d+\mu_2)+(m-\mu_1)n]^2-4[(m+\mu_1)(d+\mu_2)+z]}}{2}$ have negative real parts at infection equilibrium point, then infection equilibrium point is locally asymptotically stable whenever $R_{0V} > 1$.

Epidemiologically implying that if vibrios are introduced in a population of target cells and there are new secondary infections produced whenever $R_{0V} > 1$, then cholera disease would persist in the population of cells. The study of backward bifurcation in a disease dynamics can also occur when the reproduction number is less than unity, $R_{0V} < 1$; this is explored in the next section.

3.5.4 Bifurcation Analysis

Backward bifurcation in disease transmission models is where a stable endemic equilibrium co-exists with a stable disease-free equilibrium when the associated reproduction number is less than unity.

Investigating the nature of bifurcation involving $IFE(\frac{\Lambda}{\mu_1}, 0, 0)$ using Castilo and Song[10], consider a general system of $ODEs$ given by (3.31):

$$\frac{dx}{dt} = f(x, \psi); f : R^n \times R^n, f \in C^2(R^n \times R^n) \tag{3.31}$$

Theorem 3.5.4. *Castilo-Chavez and Song [10], we consider the following:*

(i) Let $I = D_x f(0, 0)$ is the linearization matrix of system (3.33) around the equilibrium point $x = 0$ with ψ evaluated at 0. Zero is a simple eigenvalue of the matrix I and all other eigenvalues of I have negative real parts.

(ii) Matrix I has a non-negative right eigenvector w and a left eigenvector v corresponding to the zero eigenvalue.

(iii) Let f_k denote the k^{th} component of f and

(a) $a_1 = \sum_{i,j,k=1}^{n} v_k w_i w_j \frac{\partial^2 f_k}{\partial x_i \partial x_j}(0, 0)$

(b) $a_2 = \sum_{i,k=1}^{n} v_k w_i \frac{\partial^2 f_k}{\partial x_i \partial \phi}(0, 0)$

Then the local dynamic of system (3.1) *around* $x = 0$ *is determined by* a_1 *and* a_2.

(i)If $a_1 > 0$, $a_2 > 0$. *When* $\psi < 0$, *with* $|\psi| << 1$, *then* $x = 0$ *is locally asymptotically stable and there exists a positive unstable equilibrium and when* $0 < \psi << 1$, $x = 0$ *is unstable and there exists a negative and locally asymptotically stable equilibrium.*

(ii) If $a_1 < 0$, $a_2 < 0$ *when* $\psi < 0$, *with* $|\psi| << 1$, $x = 0$ *is unstable; when* $0 < \psi << 1$, $x = 0$ *is locally asymptotically stable and there exists a positive unstable equilibrium.*

(iii)If $a_1 > 0$ *and* $a_2 < 0$ *when* $\psi < 0$, *with* $|\psi| << 1$, *then* $x = 0$ *is unstable and there exists a locally asymptotically stable negative equilibrium, when* $0 < \psi << 1$, $x = 0$ *is stable and positive unstable equilibrium appears.*

(iv)When $a_1 < 0$ *and* $a_2 > 0$ *then there exists a forward bifurcation.*

(v)When $a_1 > 0$ *and* $a_2 > 0$, *then the bifurcation at* $\psi = 0$ *is backward.*

□

Proof. Using Castilo-Chavez and Song [10], let ψ be the bifurcation parameter such that if $R_{0V} < 1$, x_0 is an IFE equilibrium for all values of ψ.

Consider

$$\frac{dx}{dt} = f(x, \psi) \tag{3.32}$$

Where f is a continuous differentiable function at least twice in both x and ψ. The IFE is the line (x_0, ψ) and local stability of the IFE changes at the point (x_0, ψ).

Let

$$B = x_1, Z = x_2, V = x_3$$

The system (3.1) becomes;

$$\begin{aligned}
\frac{dx_1(t)}{dt} &= \Lambda - (1-\gamma)\frac{\alpha x_1(t)x_3(t)}{1+\delta x_3(t)} - \mu_1 x_1(t) =: f_1 \\
\frac{dx_2(t)}{dt} &= (1-\gamma)\frac{\alpha x_1(t)x_3(t)}{1+\delta x_3(t)} - (d+\mu_2)x_2(t) =: f_2 \\
\frac{dx_3(t)}{dt} &= h_V x_2 + \beta_V V - (\sigma+s)x_3(t) =: f_3
\end{aligned} \tag{3.33}$$

Applying *Theorem* (3.5.4) to investigate if the system (3.1) exhibit a backward bifurcation. We first linearize the system and then compute its eigenvalues and eigenvectors corresponding to eigenvalues with negative real part form a basis for the stable eigenspace.

Linearizing (3.33) around the IFE yields;

$$\begin{pmatrix} -\mu_1 & 0 & \frac{-(1-\gamma)\alpha\Lambda}{\mu_1} \\ 0 & -(d+\mu_2) & \frac{(1-\gamma)\alpha\Lambda}{\mu_1} \\ 0 & h_V & \beta_V - (\sigma+s) \end{pmatrix} \tag{3.34}$$

The eigenvalue of (3.34) is given by $\lambda_1 = -\mu_1$, the trace is $-(d+\mu_2)+\beta_V-(\sigma+s)$ and the determinant $(d+\mu_2)[\beta_V-(\sigma+s)][R_{0V}-1] > 0$.

Now let $w = (w_1, w_2, w_3)^T$ be the right eigenvector for the matrix (3.35). Hence,

$$\begin{pmatrix} -\mu_1 & 0 & \frac{-(1-\gamma)\alpha\Lambda}{\mu_1} \\ 0 & -(d+\mu_2) & \frac{(1-\gamma)\alpha\Lambda}{\mu_1} \\ 0 & h_V & \beta_V - (\sigma+s) \end{pmatrix} \begin{pmatrix} w_1 \\ w_2 \\ w_3 \end{pmatrix} = 0 \tag{3.35}$$

Which yields;

$$-\frac{(1-\gamma)\alpha\Lambda}{\mu_1}w_3 = 0$$

$$-[(d+\mu_2)]w_2 + \frac{(1-\gamma)\alpha\Lambda}{\mu_1}w_3 = 0$$

$$[\beta_V - (\sigma + s)]w_3 = 0$$

Solving for w_1, w_2 and w_3, we obtain $w_1 = 2(1-\gamma)\alpha\Lambda$, $w_2 = \frac{(1-\gamma)\alpha\Lambda}{\mu_1(d+\mu_2)}$ and $w_3 = 1$. Let $v = (v_1, v_2, v_3)^T$ be the left eigenvector of equation (3.35)

$$\begin{pmatrix} -\mu_1 & 0 & 0 \\ 0 & -(d+\mu_2) & h_V \\ \frac{-(1-\gamma)\alpha\Lambda}{\mu_1} & \frac{(1-\gamma)\alpha\Lambda}{\mu_1} & \beta_V - (\sigma + s) \end{pmatrix} \begin{pmatrix} v_1 \\ v_2 \\ v_3 \end{pmatrix} = 0 \tag{3.36}$$

$$-\mu_1 v_1 = 0$$

$$-[(d+\mu_2)]v_2 = 0$$

$$[\frac{-(1-\gamma)\alpha\Lambda}{\mu_1}]v_1 + [\frac{(1-\gamma)\alpha\Lambda}{\mu_1}]v_2 + [\beta_V - (\sigma + s)]v_3 = 0$$

Solving for v_1, v_2 and v_3 we obtain $v_1 = 0$, $v_2 = 0$ and $v_3 = 1$.

It is observed that $v.w = 1$. Now, evaluating the partial derivatives of system (3.34) at IFE yields;

$$\frac{\partial^2 f_1}{\partial x_1 \partial x_3} = \frac{\partial^2 f_1}{\partial x_3 \partial x_1} = \frac{-(1-\gamma)\alpha}{\delta}$$

$$\frac{\partial^2 f_2}{\partial x_1 \partial x_3} = \frac{(1-\gamma)\alpha}{\delta}$$

□

We therefore note that all the other second order partial derivatives are equal to zero. Thus, computing the coefficients a_1 and a_2 defined in *Theorem* 3.5.4.

$$a_1 = \sum_{i,j,k=1}^{n} v_k w_i w_j \frac{\partial^2 f_k}{\partial x_i \partial x_j}$$

$$a_2 = \sum_{i,k=1}^{n} v_k w_i \frac{\partial^2 f_k}{\partial x_i \partial x_j}$$

Consider the system (3.33) and considering a_1 and a_2 only as the non-zero derivatives for the terms $\frac{\partial^2 f_k}{\partial x_i \partial x_j}$ and $\frac{\partial^2 f_k}{\partial x_i \partial x_j}$ it follows that;

$$a_1 = 2v_3 w_1 w_3 \frac{\partial^2 f_2}{\partial x_1 \partial x_3} + v_3 w_2 w_1 \frac{\partial^2 f_1}{\partial x_3 \partial x_1}$$

$$a_2 = v_3 w_1 \frac{\partial^2 f_2}{\partial x_1 \partial x_3} + v_3 w_2 \frac{\partial^2 f_2}{\partial x_1 \partial x_3} + v_3 w_3 \frac{\partial^2 f_2}{\partial x_1 \partial x_3} \tag{3.37}$$

Substituting v_s and w_s in (3.37) yields

$$a_1 = 2\frac{(1-\gamma)^2 \alpha^2 \Lambda}{\delta}$$
$$a_2 = \frac{(1-\gamma)\alpha}{\delta}[1 + \frac{(1-\gamma)\alpha\Lambda}{\mu_1(d+\mu_2)} + 2(1-\gamma)\alpha\Lambda]$$

The signs of coefficients a_1 and a_2 determine the nature of bifurcation exhibited by system (3.1). For model (3.1) to undergo backward bifurcation, then $a_1 > 0$ and $a_2 > 0$. Consider the parameter values used in *Table* 3.1 to verify the conditions $a_1 > 0$ and $a_2 > 0$ where

$$a_1 = 2\frac{(1-\gamma)^2 \alpha^2 \Lambda}{\delta}$$
$$a_2 = \frac{(1-\gamma)\alpha}{\delta}[1 + \frac{(1-\gamma)\alpha\Lambda}{\mu_1(d+\mu_2)} + 2(1-\gamma)\alpha\Lambda]$$

Let $\alpha = 0.09$, $\gamma = 0.9$, $\delta = 0.05$, $\mu_1 = \mu_2 = 0.27$ substituting these numerical values in a_1 and a_2 yields $a_1 > 0 = 3.24 \times 10^3$ and $a_2 > 0 = 2.68304 \times 10^5$. Hence, model (3.1) exhibits backward bifurcation. This implies the epidemiological implication in relation to cholera disease of backward bifurcation is that $R_{0V} < 1$ is necessary and not sufficient for effective control of cholera disease; hence in a backward bifurcation setting the cholera disease will invade to a relatively high endemic level in cells.

3.6 Numerical Simulation

In this section, numerical simulation is done to illustrate the theoretical results by numerically solving the model system (3.1). This is carried out by first taking the initial values from existing literature as shown in *Table* 1. Using the parameter values in *Table* (1) and fitting the model (3.1) in MATLAB software, the *ode*45 command in $MATLAB$ is used to solve it and the results in Section (3.6.2) are obtained.

3.6.1 Parameter Values

The parameters values are described in Table (3.1).

Table 3.1: Parameter values for the within-host cholera Model

Description	Parameters	Initial value	Source
Recruitment rate of B	Λ	$1.0 * 10^6$ *cells*	[37]
Natural death rate of B	μ_1	0.27 day^{-1}	[12]
Natural death rate of Z	μ_2	0.27 day^{-1}	[12]
Contact rate of B and V	α	0.9 day^{-1}	[12]
Clearance rate of V	σ	0.02 day^{-1}	[12]
Vaccine Efficacy	γ	0.66	[39]
Recruitment rate of V	h_V	0.7 day^{-1}	[37]
Shedding rate of V	s	0.03 day^{-1}	[37]
Multiplication rate of V	β_V	0.3 day^{-1}	[37]

3.6.2 Simulation Results

The graphs and the results obtained are described as in the *Figures* 3.1, *Figure* 3.2, *Figure* 3.3 and *Figure* 3.4 .

Figure 3.1, *Figure* 3.2, *Figure* 3.3 and *Figure* 3.4 shows a graph of target cells B, infected cells Z and the vibrio V against time in minutes when $\gamma = 0.1$, when $\gamma = 0.6$ and when $\gamma = 0.9$ respectively.

In *Figure* 3.1, it is observed that if the vaccine efficacy is low i.e $\gamma = 0.1$, there are more cells infected which is an indication that there are pathogens invading the target cells in the small intestine as a result decrease in number of target cells as they become infected due to their interaction with the pathogen. This implies that the lower the vaccine efficacy, the higher the rate of infection of target cells.

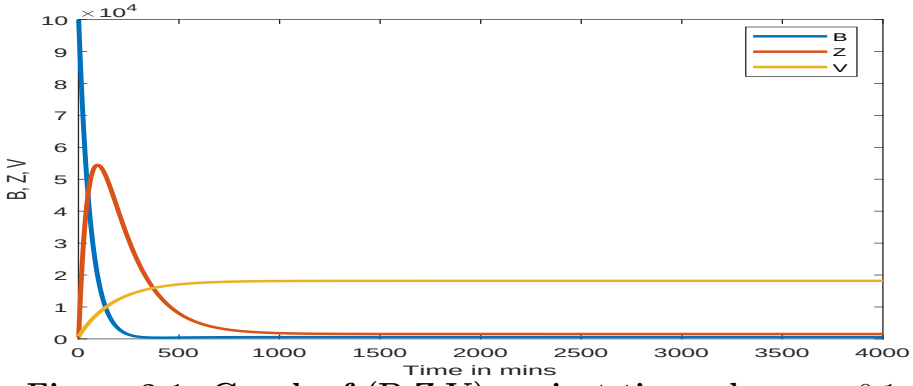

Figure 3.1: Graph of (B,Z,V) against time when $\gamma = 0.1$

In *Figure* 3.2, the vaccine efficacy is $\gamma = 0.6$, the number of cells infected decreases compared to when $\gamma = 0.1$. This shows that with improved vaccine efficacy there will be low infection of cells without which the vibrios will continue to invade the cells to cause infection and this explains why cholera disease is persistence.

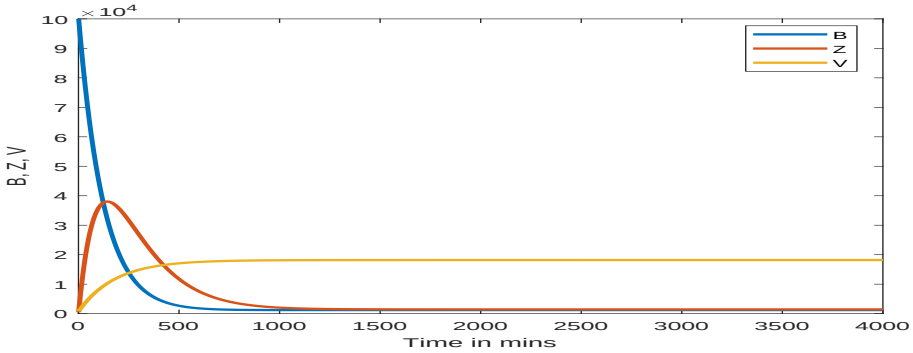

Figure 3.2: Graph of (B,Z,V) against time when $\gamma = 0.6$

In *Figure* 3.3, the vaccine efficacy is $\gamma = 0.9$, this leads to decrease in the number of cells infected which implies that with vaccine efficacy being high, the chances of cells getting infected will be low compared to when the vaccine efficacy is low. It also implies that when the vaccine efficacy is high, it takes longer time for healthy cells to be infected.

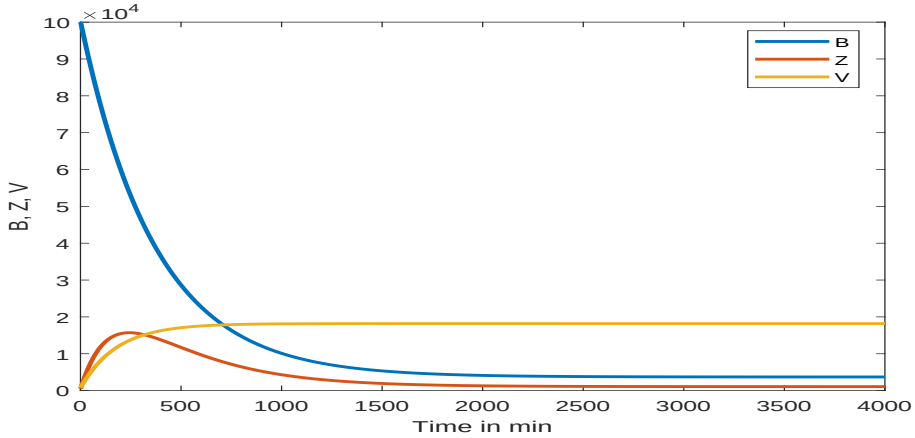

Figure 3.3: Graph of (B,Z,V) against time when $\gamma = 0.9$

Figure 3.4 shows backward bifurcation diagram for the force of infection against reproduction number of model (3.1) using parameter values $\alpha = 0.9$, $\gamma = 0.66$, $\delta = 0.05$, $d = 0.4$ and $\mu_1 = \mu_2 = 0.27$. This shows that backward bifurcation occurs for values of R_{0V} such that $R_0^* < R_{0V} < 1$ hence, reoccurrence of in-host infection cholera disease when $R_{0V} < 1$.

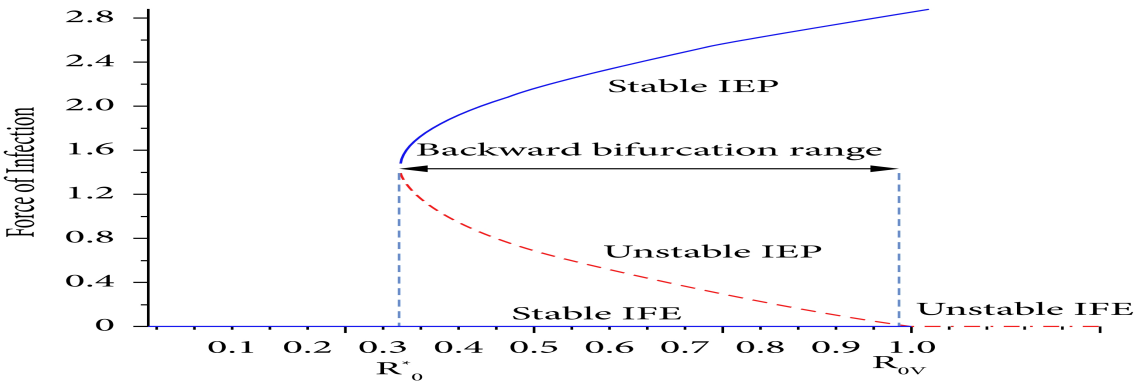

Figure 3.4: Bifurcation Analysis Curve

3.7 Conclusion

In this research, a within-host cholera model with vaccination is developed and analysed. The existence and stability of the steady states of the model has been determined and show that it is locally and globally asymptotically stable when $R_{0V} < 1$ and unstable when $R_{0V} > 1$. The analysis of the model also show that infection equilibrium point is locally asymptotically stable when $R_{0V} > 1$; this means that there is persistent infection. Furthermore, analysis shows that when the vaccine efficacy γ is high, there is high clearance rate of Z and V. In this research, $R_{0V} < 1$ is not sufficient enough to eradicate in-host cholera disease; as a result, the model (3.1) undergoes backward bifurcation indicating co-existence of infection free equilibrium point and infection equilibrium point when $R_{0V} < 1$ and this explains why cholera disease has remained persistently endemic.

CHAPTER FOUR

DYNAMICS OF BETWEEN-HOST CHOLERA MODEL WITH TEMPERATURE DEPENDENT PARAMETER

4.1 Introduction

Many studies have been done to determine the dynamics of weather conditions (rain/drought) on the spread of cholera disease but none has been done to determine the dynamics of temperature on the multiplication and spread of *Vibrio cholerae*. In the previous model of within-host cholera disease with vaccination analysed in Chapter 3, it has been shown that despite vaccination against cholera backward bifurcation occurs even when $R_{0V} < 1$. It therefore means that *Vibrio cholerae* still exists in the human small intestine and is thus released to the environment through defaecation or is spread between human beings. From research [32], the normal standard state environmental temperature is in the range 20.0^0C to 25.0^0C and the average axillary body temperature is 37.0^0C, with the upper limit of normal defined as 38.0^0C and the typical temporary elevations in body temperature ranging from 38.0^0C to 40.0^0C caused by most short-lived (acute) infections. Studies [15] have shown that cholera incidence have been predominant when there is always interchange of seasons hence making it difficult in controlling cholera disease. In this study a between-host cholera model with temperature dependent parameter is formulated and analysed to investigate the effect of temperature change on the dynamics of between-host cholera disease.

In section (4.2) the model is described and formulated, in section (4.3) positivity and boundedness of solutions of the model are investigated, in section (4.4) the basic reproduction number is determined, in section (4.5) stability analysis at the

equilibrium points are analysed, in section (4.6) sensitivity analysis is performed to examine the effect of changes in the model's parameter and in section (4.7) numerical simulation of the formulated model is done to investigate the effect of the temperature of the environment on the dynamics of cholera disease.

4.2 Model Description and Formulation

The human population is divided into Susceptible individuals $S(t)$, Infected individuals $I(t)$ and the Removed individuals $R(t)$. The vibrio concentration is denoted by $B(t)$. Susceptible individuals are recruited at a constant rate Λ_1. The population of the susceptible individuals is reduced by infection resulting from interaction with the *Vibrio cholerae* in the environment at contact rate θ. The transmission rates when susceptible interacts with the pathogens is controlled by ω. This population of susceptible is reduced through oral vaccination at the rate v. The vaccine administered presently are not perfect, some have efficacy as low as 65 percent [39]. Therefore, it is likely that vaccinated individuals can acquire infection. The population of vaccinated removed individuals is given by ρvS, where ρ is the fraction of vaccinated individuals who don't get infected and vS is the total vaccinated population. $(1-\rho)vS$ is the population of vaccinated individuals who can be infected.

In formulation of this model, the temperature of the environment is considered as a determining factor to the multiplication of *Vibrio cholerae* and its ability to cause infection hence, the temperature dependent parameter $\alpha_1(T)$ is incorporated in the transmission route. The population of infected individuals resulting from the interaction between the susceptible individuals and the pathogen in the environment is given by $\omega\theta\frac{SB\alpha_1(T)}{K+B}$.

$\frac{\omega\theta_1(1-\rho)vSB\alpha_1(T)}{K+B}$ is the proportion of those vaccinated and infected from interacting with the pathogens from the environment, where θ_1 accounts for the fact that the transmission probability for the vaccinated group is less than unvaccinated group. The infected population is reduced by the death due to infection at the rate σ and natural death the rate μ and recovery from the infection at the rate γ_1. The carrying capacity of vibrios is given by K. Susceptible population is reduced by natural death at the rate μ. The concentration of the vibrio is generated at the rate ϵ through the action of the infected individuals [39] and is decreased by natural death at the rate μ_1.

The system of ordinary differential equation governing the description previously is as follows:

$$\begin{aligned}
\frac{dS}{dt} &= \Lambda_1 - \frac{\omega\theta SB\alpha_1(T)}{K+B} - \frac{\omega\theta_1(1-\rho)vSB\alpha_1(T)}{K+B} - \mu S - \rho vS \\
\frac{dI}{dt} &= \frac{\omega\theta SB\alpha_1(T)}{K+B} + \frac{\omega\theta_1(1-\rho)vSB\alpha_1(T)}{K+B} - (\gamma_1 + \epsilon + \mu + \sigma)I \\
\frac{dR}{dt} &= \gamma_1 I + \rho vS - \mu R \\
\frac{dB}{dt} &= \epsilon I - \mu_1 B
\end{aligned} \tag{4.1}$$

4.2.1 Assumptions of the Model.

The model considers infection due to interaction with the pathogen from the environment.

4.3 Positivity and Boundedness of the Model.

Since model (4.1) describes human population, it should be well posed. Thus in this section, positivity and boundedness solutions of model (4.1) is discussed. Since equation (4) of model (4.1) is the equation of the pathogen class, it shall not

be considered in the analysis.

Positivity of solutions of the model(4.1) is determined using the following initial conditions (4.2);

$$S(0) = S_0 \geq 0, I(0) = I_0 \geq 0, R(0) = R_0 \geq 0, B(0) = B_0 \geq 0. \tag{4.2}$$

4.3.1 Positivity of the Model

In this section, initial conditions (4.2) is used to show that the solutions for model (4.1) are positive in region defined by ψ.

Proposition 4.3.1. *Solutions of model (4.1) with initial condition (4.2) are positive in the region defined as* $\psi = (S, I, R) \in \mathbb{R}^3_+ \times \mathbb{R}$

Proof. From Proposition (4.3.1) the solutions of model (4.1) given the initial condition (4.2) are positive for all $t \geq 0$. Consider the first equation of model (4.1) given by;

$$\frac{dS}{dt} = \Lambda_1 - \frac{\omega\theta SB\alpha_1(T)}{K+B} - \frac{\omega\theta_1(1-\rho)vSB\alpha_1(T)}{K+B} - \mu S - \rho vS \tag{4.3}$$

$$> -\{\frac{\omega\theta B\alpha_1(T)}{K+B} + \frac{\omega\theta_1(1-\rho)vB\alpha_1(T)}{K+B} + \mu + \rho v\}S$$

This results in $S(t) > S_0 e^{-\int_0^t [\frac{\omega\theta B\alpha_1(T)}{K+B} + \frac{\omega\theta_1(1-\rho)vB\alpha_1(T)}{K+B} + \mu + \rho v]dt} > 0$

This implies that $S(t) > 0$.

In a similar manner, the second equation of model (4.1) given by;

$$\frac{dI}{dt} = \frac{\omega\theta SB\alpha_1(T)}{K+B} + \frac{\omega\theta_1(1-\rho)vSB\alpha_1(T)}{K+B} - (\gamma_1 + \epsilon + \mu + \sigma)I$$

$$> -(\gamma_1 + \epsilon + \mu + \sigma)I$$

This results in $I(t) > I_0 e^{-\int_0^t (\gamma_1+\epsilon+\mu+\sigma)dt} > 0$

This implies that $I(t) > 0$.

The third equation of model (4.1) given by;

$$\frac{dR}{dt} = \gamma_1 I + \rho v S - \mu R$$

Which results in $R(t) = R_0 e^{-\int_0^t (\mu)dt} > 0$

This implies that $R(t) > 0$.

Therefore $(S, I, R) \in \mathbb{R}^3_+$ is a positive invariant set for the system of equation (4.1). Hence, with positive initial conditions (4.2), the solutions of model (4.1) are all positive. □

4.3.2 Boundedness of the Model

Since the model formulated describes human population, the population will always remain bounded.

Proposition 4.3.2. *Let $t_0 > 0$. If $S_0 > 0$, $I_0 > 0$ and $R_0 > 0$ then $S(t)$, $S(t)$ and Rt) in model (4.1) will remain bounded in $\in \mathbb{R}^3$ for all $t \in [0, t_0]$.*

Proof. Let $N(t) := S(t) + I(t) + R(t)$ be the total number of human population. From the system of equation (4.1);

$$N'(t) \leq \Lambda_1 - \mu(S + I + R) \leq \Lambda_1 - \mu N(t)$$

$$N'(t) \leq \Lambda_1 - \mu N(t)$$

Integrating both sides of $N'(t) \leq \Lambda_1 - \mu N(t)$ with respect to (t) given by;

$$\int N'(t)dt \leq \int (\Lambda_1 - \mu N(t))dt$$

$$N(t)e^{\mu t} \leq \int \frac{\Lambda_1}{\mu} e^{\mu t} dt$$

Integrating the right side of $N(t)e^{\mu t} \leq \int \frac{\Lambda_1}{\mu} e^{\mu t} dt$ with respect to (t) yields

$$N(t)e^{\mu t} \leq \frac{\Lambda_1}{\mu^2} e^{\mu t} + C$$

$$N(t) \leq \frac{\Lambda_1}{\mu^2} + Ce^{-\mu t}$$

$$\lim_{t \to \infty} N(t) \leq \frac{\Lambda_1}{\mu^2}$$

Hence $N(t)$ is bounded. From *Proposition* (4.3.1) and (4.3.2), solutions of model (4.1) are positive and bounded for $t \geq 0$. Hence, the model (4.1) is mathematically and epidemiologically meaningful to consider its solutions in ψ. □

4.4 Basic Reproduction Number, R_0.

Definition 4.4.1. *The basic reproduction number* (R_0) *is the number of secondary infections resulting from the introduction of an infective individual into a population of susceptible individuals.*

Applying the method of next generation matrix approach given by [38] to determine the basic reproduction number R_0. Consider the matrix

$$FV^{-1}.$$

Where F is the jacobian of $\mathcal{F}$ which refers to the rate of new infection and V is the Jacobian of $\mathcal{V}$ which is the matrix for the transition terms. From model (4.1) the associated matrices are;

$$\mathcal{F} = \begin{pmatrix} \frac{\omega\theta SB\alpha_1(T)}{K+B} + \frac{\omega\theta_1(1-\rho)vSB\alpha_1(T)}{K+B} \\ 0 \end{pmatrix} \tag{4.4}$$

$$\mathcal{V} = \begin{pmatrix} (\gamma_1 + \epsilon + \mu + \sigma)I \\ \mu_1 B - \epsilon I \end{pmatrix} \tag{4.5}$$

The reproduction number $R_0 = \eta(FV^{-1})$ is the spectral radius of the matrix FV^{-1}. Therefore;

$$R_0 = \epsilon[\frac{\omega\theta\Lambda_1\alpha_1(T) + \omega\theta_1(1-\rho)v\Lambda_1\alpha_1(T)}{K\mu_1(\mu+\rho v)(\gamma_1+\epsilon+\mu+\sigma)}] \tag{4.6}$$

Since R_0 is a measure of the severity of an epidemic, it determines whether the disease will invade in a population or not. Epidemiologically, this implies that if $R_0 < 1$ the infection dies out and if $R_0 > 1$ the disease persist in the population.

4.5 Stability Analysis

In this section the stability analysis of the equilibria points is carried out to predict the long term behaviour of the solutions of the model (4.1).

4.5.1 Existence of Disease Free Equilibrium (DFE) Point

These are steady state solutions in absence of cholera disease, hence $I = B = 0$.

Proposition 4.5.1. *For the model (4.1) there always exists a DFE point denoted* (S^0, I^0, R^0, B^0).

Proof. At the equilibrium point, the rate of change of the model equations (4.1) are assumed to be zero. Therefore

$$\Lambda_1 - \frac{\omega\theta SB\alpha_1(T)}{K+B} - \frac{\omega\theta_1(1-\rho)vSB\alpha_1(T)}{K+B} - \mu S - \rho v S = 0$$

$$\frac{\omega\theta SB\alpha_1(T)}{K+B} + \frac{\omega\theta_1(1-\rho)vSB\alpha_1(T)}{K+B} - (\gamma_1+\epsilon+\mu+\sigma)I = 0$$

$$\gamma_1 I + \rho v S - \mu R = 0$$

$$\epsilon I - \mu_1 B = 0$$

Since at DFE the infection compartments are zero, let $I = 0$ and $B = 0$. Substituting $I = 0$, $B = 0$ into the above equations yield;

$$\Lambda_1 - \rho v S - \mu S = 0$$

$$\rho v S - \mu R = 0$$

Solving the above equations yields

$$S = \frac{\Lambda_1}{(\mu + \rho v)}$$

$$I = 0$$

$$B = 0$$

$$R = \frac{\rho v \Lambda_1}{\mu(\mu + \rho v)}$$

Therefore the DFE points of model system (4.1) is given by;

$$(S^0, I^0, R^0, B^0) = (\frac{\Lambda_1}{(\mu + \rho v)}, 0, \frac{\rho v \Lambda_1}{\mu(\mu + \rho v)}, 0)$$

This shows that there is no infection in the DFE of the model (4.1). □

4.5.2 Local Stability of the Disease Free Equilibrium (DFE)

Theorem 4.5.1. *For any time $t \geq 0$, the disease free equilibrium points of model (4.1) is locally asymptotically stable when $R_0 < 1$ and unstable when $R_0 > 1$.*

Proof. The jacobian matrix of (4.1) is as follows;

$$J = \begin{pmatrix} -\frac{\omega\theta B\alpha_1(T)}{K+B} - \frac{\omega\theta_1(1-\rho)vB\alpha_1(T)}{K+B} - \mu - \rho v & 0 & 0 & u \\ \frac{\omega\theta B\alpha_1(T)}{K+B} + \frac{\omega\theta_1(1-\rho)vB\alpha_1(T)}{K+B} & -(\gamma_1+\epsilon+\mu+\sigma) & 0 & g \\ \rho v & \gamma_1 & -\mu & 0 \\ 0 & \epsilon & 0 & -\mu_1 \end{pmatrix} \tag{4.7}$$

where $u = -\frac{\omega\theta SK\alpha_1(T)}{(K+B)^2} - \frac{\omega\theta_1(1-\rho)vSK\alpha_1(T)}{(K+B)^2}$ and $g = \frac{\omega\theta SK\alpha_1(T)}{(K+B)^2} + \frac{\omega\theta_1(1-\rho)vSK\alpha_1(T)}{(K+B)^2}$

Substituting the DFE point in the jacobian matrix of (4.1) yields;

$$J_{DFE} = \begin{pmatrix} -\mu-\rho v & 0 & 0 & -\frac{\omega\theta\frac{\Lambda_1}{(\mu+\rho v)}\alpha_1(T)}{K} - \frac{\omega\theta_1(1-\rho)v\frac{\Lambda_1}{(\mu+\rho v)}\alpha_1(T)}{K} \\ 0 & -(\gamma_1+\epsilon+\mu+\sigma) & 0 & \frac{\omega\theta\frac{\Lambda_1}{(\mu+\rho v)}\alpha_1(T)}{K} + \frac{\omega\theta_1(1-\rho)v\frac{\Lambda_1}{(\mu+\rho v)}\alpha_1(T)}{K} \\ \rho v & \gamma_1 & -\mu & 0 \\ 0 & \epsilon & 0 & -\mu_1 \end{pmatrix} \tag{4.8}$$

For asymptotic stability all the eigenvalues should be strictly real and negative. It can be seen clearly from (4.8) that $\lambda_1 = -\mu$ and $\lambda_2 = -\mu - \rho v$.

For local asymptotic stability consider Jordan block 2×2 matrix (4.9) to determine the negative trace and conditions for positive determinant.

$$\begin{pmatrix} -(\gamma_1+\epsilon+\mu+\sigma) & \frac{\omega\theta\frac{\Lambda_1}{(\mu+\rho v)}\alpha_1(T)}{K} + \frac{\omega\theta_1(1-\rho)v\frac{\Lambda_1}{(\mu+\rho v)}\alpha_1(T)}{K} \\ \epsilon & -\mu_1 \end{pmatrix} \tag{4.9}$$

From (4.9) the trace is $-(\gamma_1+\epsilon+\mu+\sigma) - \mu_1$

Determinant;

$$(\gamma_1+\epsilon+\mu+\sigma)\mu_1 - \epsilon[\frac{\omega\theta\frac{\Lambda_1}{(\mu+\rho v)}\alpha_1(T)}{K} + \frac{\omega\theta_1(1-\rho)v\frac{\Lambda_1}{(\mu+\rho v)}\alpha_1(T)}{K}]$$

This determinant is written as $[(\gamma_1+\epsilon+\mu+\sigma)\mu_1]R_0 = \epsilon[\frac{\omega S\alpha_1(T)[\theta+\theta_1(1-\rho)v}{K}]$

This is equivalent to $[(\gamma_1+\epsilon+\mu+\sigma)][1-R_0]$, hence the determinant will be positive if $R_0 < 1$. Hence all the roots are real and negative, it implies that DFE is locally asymptotically stable whenever $R_0 < 1$, otherwise unstable.

This implies that a small perturbation of the DFE, the solutions of model (4.1) will eventually converge to DFE whenever $R_0 < 1$.

Epidemiologically this implies that if a few infectious individuals are introduced into a fully susceptible population, then there is a high chance of infecting less than one individual in its entire period of infectivity, this implies that cholera disease would die out whenever $R_0 < 1$, otherwise the disease would spread.

□

4.5.3 Global Stability of the Disease Free Equilibrium (DFE)

In this section, the global asymptotic stability of the DFE of the model (4.1) is explored. Using the Matrix theoretic method; let

$$f(x, y) = (F - V)x - \mathcal{F}(x, y) + \mathcal{V}(x, y)$$

Then $x^{'} = (F - V)x - \mathcal{F}(x, y)$

Now let $f(0, y) = 0$ and $\omega^T \geq 0$ be the left eigenvector of the nonnegative $V^{-1}F$ corresponding to the eigenvalue $\rho V^{-1}F = \rho F V^{-1} = R_0$. Therefore the following results provide a general method to construct Lyapunov function for $x^{'} = (F - V)x - \mathcal{F}(x, y)$. This type of Lyapunov function has previously been used to study the global dynamics for disease models for instance [22] [23].

Theorem 4.5.2. *Let F, V and $f(x, y)$ be defined as in $f(x, y) = (F - V)x - \mathcal{F}(x, y) + \mathcal{V}(x, y)$ and $F = [\frac{\partial F_i}{\partial x_j}(0, y_0)]$ and $V = [\frac{\partial V_i}{\partial x_j}(0, y_0)]$ respectively. If $f(x, y) \geq 0$ in $\Gamma \subset \mathbb{R}^{n+m}_{+}$, $F \geq 0$, $V^{-1} \geq 0$ and $R_0 \leq 1$, then the function $C = \omega^T V^{-1} x$ is a Lyapunov function on Γ.*

Proof. From model (4.1)

$$\mathcal{F} = \begin{pmatrix} \frac{\omega\theta SB\alpha_1(T)}{K+B} + \frac{\omega\theta_1(1-\rho)vSB\alpha_1(T)}{K+B} \\ 0 \end{pmatrix} \tag{4.10}$$

and

$$\mathcal{V} = \begin{pmatrix} (\gamma_1 + \epsilon + \mu + \sigma)I \\ \mu_1 B - \epsilon I \end{pmatrix} \tag{4.11}$$

Differentiating C along solution of

$$x^{'} = \mathcal{F}(x,y) - \mathcal{V}(x,y), y^{'} = g(x,y)$$

Gives;

$$C^{'} = C^{'}|_{(x'=\mathcal{F}(x,y)-\mathcal{V}(x,y),y'=g(x,y))} = \omega^T V^{-1} x^{'} = \omega^T V^{-1}(F-V)x - \omega^T V^{-1} f(x,y)$$

$$= (R_0 - 1)\omega^T x - \omega^T V^{-1} f(x,y)$$

Since $\omega^T \geq 0$, $V^{-1} \geq 0$ and $f(x,y) \geq 0$ in Γ, then the last term is nonpositive.

If $R_0 \leq 1$, then $C^{'} \leq 0$ in Γ and therefore C is a Lyapunov function for $x^{'} = \mathcal{F}(x,y) - \mathcal{V}(x,y)$. □

Theorem 4.5.3. *Let F, V and $f(x,y)$ be defined as in $f(x,y) = (F-V)x - \mathcal{F}(x,y) + \mathcal{V}(x,y)$ and $F = [\frac{\partial F_i}{\partial x_j}(0,y_0)]$ and $V = [\frac{\partial V_i}{\partial x_j}(0,y_0)]$ respectively. Suppose that $f(x,y) \geq 0$ with $f(x,y_0) = 0$ in Γ, $F \geq 0$, $V^{-1} \geq 0$ and $V^{-1}F$ is irreducible. Assuming that the DFE system $y^{'} = g(0,y)$ has a unique equilibrium $y = y_0 > 0$ that is globally asymptotically stable in $\mathbb{R}^m_+$. Then the following results holds for $x^{'} = \mathcal{F}(x,y) - \mathcal{V}(x,y), y^{'} = g(x,y)$.*

(i) If $R_0 < 1$ then the DFE is globally asymptotically stable in Γ

(ii) If $R_0 > 1$ then the DFE is unstable and the system $x^{'} = \mathcal{F}(x,y) - \mathcal{V}(x,y), y^{'} = g(x,y)$ is uniformly persistent and there exists at least one EE

Proof. By *Theorem* (4.5.2), $C = \omega^T V^{-1} x$ is a Lyapunov function for $x^{'} = \mathcal{F}(x, y) - \mathcal{V}(x, y), y^{'} = g(x, y)$ provided $R_0 < 1$. Since $V^{-1}F$ is irreducible , it follows that $\omega > 0$.

Hence by $(R_0 - 1)\omega^T x - \omega^T V^{-1} f(x, y)$, $C^{'} = 0$ implying that $\omega^T x = 0$ and thus $x = 0$.

Using the global stability assumption for the disease free system and the fact that $f(0, y) = 0$, the only invariant set in $\mathbb{R}^{n+m}{}_+$ where $x = 0$ is the singleton P_0. By Lasalle's invariance principle [25], P_0 is globally asymptotically stable in Γ.

If $R_0 > 1$, then by $(R_0 - 1)\omega^T x - \omega^T V^{-1} f(x, y)$, $C^{'} = (R_0 - 1)\omega^T x > 0$ provided $x > 0$ and $y = y_0$. By continuity $C^{'} > 0$ in a neighborhood of P_0. Therefore, solutions in the positive cone sufficiently close to P_0 move away from P_0, this implies that P_0 is unstable.

Epidemiologically implying that if a large number of infectious individuals are introduced into a fully susceptible population, the disease would die off if there are no secondary infections produced whenever $R_0 < 1$, otherwise the disease would spread. □

4.5.4 Local Stability of the Endemic Equilibrium (EE) Points

This is the state in which all the compartments of the model (4.1) are non-zero. To obtain the EE points, the model (4.1) is solved simultaneously.

Theorem 4.5.4. *The endemic equilibrium point $EE^*(S^*, I^*, R^*, B^*)$ of model (4.1) is locally asymptotically stable whenever $R_0 > 1$.*

Proof. When the system of equations in model system (4.1) is equated to zero we obtain;

$$\Lambda_1 - \frac{\omega\theta SB\alpha_1(T)}{K+B} - \frac{\omega\theta_1(1-\rho)vSB\alpha_1(T)}{K+B} - \mu S - \rho vS = 0$$

$$\frac{\omega\theta SB\alpha_1(T)}{K+B} + \frac{\omega\theta_1(1-\rho)vSB\alpha_1(T)}{K+B} - (\gamma_1 + \epsilon + \mu + \sigma)I = 0$$

$$\gamma_1 I + \rho vS - \mu R = 0$$

$$\epsilon I - \mu_1 B = 0$$

Solving for B^* yields;

$$B^* = (\frac{\epsilon I^*}{\mu_1})$$

Solving for R^* yields;

$$R^* = (\frac{\gamma_1^* + \rho vS^*}{\mu})$$

Solving for S^* yields;

$$S^* = \frac{\Lambda_1}{\mu + \rho v + \frac{\omega\theta\epsilon\alpha_1(T)}{K+\frac{\epsilon I^*}{\mu}} + \frac{\omega\theta_1(1-\rho)v\epsilon\alpha_1(T)}{K+\frac{\epsilon I^*}{\mu}}}$$

Solving for I^* yields;

$$I^* = \frac{\omega\theta\epsilon S^*\alpha_1(T)}{(K+\frac{\epsilon I^*}{\mu})(\gamma_1+\epsilon+\mu+\sigma)} + \frac{\omega\theta_1(1-\rho)\epsilon S^*\alpha_1(T)}{(K+\frac{\epsilon I^*}{\mu})(\gamma_1+\epsilon+\mu+\sigma)}$$

The jacobian matrix of (4.1) in terms of (S^*, I^*, R^*, B^*) is given by

$$J_{EE^*} = \begin{pmatrix} -q & 0 & 0 & -\frac{\omega\theta S^*K\alpha_1(T)}{(K+B^*)^2} - \frac{\omega\theta_1(1-\rho)vS^*K\alpha_1(T)}{(K+B^*)^2} \\ l & -(\gamma_1+\epsilon+\mu+\sigma) & 0 & \frac{\omega\theta S^*K\alpha_1(T)}{(K+B^*)^2} + \frac{\omega\theta_1(1-\rho)vS^*K\alpha_1(T)}{(K+B^*)^2} \\ \rho v & \gamma_1 & -\mu & 0 \\ 0 & \epsilon & 0 & -\mu_1 \end{pmatrix} \tag{4.12}$$

let $q = \frac{\omega\theta B^*\alpha_1(T)}{K+B^*} + \frac{\omega\theta_1(1-\rho)vB^*\alpha_1(T)}{K+B^*} + \mu + \rho v$ and $l = \frac{\omega\theta B^*\alpha_1(T)}{K+B^*} + \frac{\omega\theta_1(1-\rho)vB^*\alpha_1(T)}{K+B^*}$

To find the eigenvalues, consider the characteristics equation

$$| \lambda I - J_{EE^*} | = 0$$

Yields;

$$\begin{vmatrix} -q-\lambda & 0 & 0 & -\frac{\omega\theta S^*K\alpha_1(T)}{(K+B^*)^2} - \frac{\omega\theta_1(1-\rho)vS^*K\alpha_1(T)}{(K+B^*)^2} \\ l & -(\gamma_1+\epsilon+\mu+\sigma)-\lambda & 0 & \frac{\omega\theta S^*K\alpha_1(T)}{(K+B^*)^2} + \frac{\omega\theta_1(1-\rho)vS^*K\alpha_1(T)}{(K+B^*)^2} \\ \rho v & \gamma_1 & -\mu-\lambda & 0 \\ 0 & \epsilon & 0 & -\mu_1-\lambda \end{vmatrix} = 0 \tag{4.13}$$

From (4.13) which can be written as $(\lambda+\mu)(\lambda+\mu_1)(\lambda^2+b\lambda+c) = 0$

Where

$$b = -[\frac{\omega\theta B^*\alpha_1(T)}{K+B^*} + \frac{\omega\theta_1(1-\rho)vB^*\alpha_1(T)}{K+B^*} + \mu + \rho v] - [(\gamma_1+\epsilon+\mu+\sigma)]$$

And

$$c = [\frac{\omega\theta B^*\alpha_1(T)}{K+B^*} + \frac{\omega\theta_1(1-\rho)vB^*\alpha_1(T)}{K+B^*} + \mu + \rho v][(\gamma_1+\epsilon+\mu+\sigma)]$$

It implies that $\lambda_1 = -\mu$ and $\lambda_2 = -\mu_1$. Hence it can clearly be seen that $\lambda_1 = -\mu$, $\lambda_2 = -\mu_1$ are negative.

To find the remaining eigenvalues of (4.13), let $\lambda^2 + b\lambda + c = 0$ such that

When $\lambda^2 + b\lambda + c = 0$ is solved yield $b = \lambda_3 + \lambda_4$ and $c = \lambda_3\lambda_4$. Hence whenever $R_0 < 1$, then $[\frac{\omega\theta B^*\alpha_1(T)}{K+B^*} + \frac{\omega\theta_1(1-\rho)vB^*\alpha_1(T)}{K+B^*} + \mu + \rho v] < [(\gamma_1+\epsilon+\mu+\sigma)]$. If $\rho v < \mu$ then $b > 0$, $c > 0$. Therefore, $\lambda_3 < 0$, $\lambda_4 < 0$. Therefore all the roots are real and negative and EE^* is locally asymptotically stable whenever $R_0 > 1$, otherwise unstable.

Theorem (4.5.4) implies that a small perturbation of the EE, the solutions of the model (4.1) will always converge to the EE whenever $R_0 > 1$.

This implies that if a few infectious individuals are introduced into a fully susceptible population and there are new secondary infections produced whenever $R_0 > 1$, then the disease would persist in the population. □

4.6 Sensitivity Analysis

Sensitivity analysis is the degree to which an input parameter to a model affects the output. This analysis is performed to examine the effect of changes in the model's parameter to the dynamics of the models' compartment. This parameters have a significant impact on the dynamics of disease transmission [31]. Using the normalized forward sensitivity index of a variable to a parameter which is the ratio of the relative change in the parameter, this variable is a differential function of the parameter [31]. The sensitivity index is therefore defined using partial derivatives.

Definition 4.6.1. *The normalized forward sensitivity index of a variable R_0 that depend differentiability on a parameter p is defined by;*

$$\theta_p^{R_0} = \frac{\partial R_0}{\partial p}\frac{p}{R_0}$$

p is the parameter whose sensitivity index is to be measured [31].

There is need to investigate the sensitivity indices of the basic reproduction number R_0, relative to the parameters involved. The basic reproduction number of the model 4.1 is given by;

$$R_0 = \epsilon[\frac{\omega\theta\Lambda_1\alpha_1(T) + \omega\theta_1(1-\rho)v\Lambda_1\alpha_1(T)}{K\mu_1(\mu+\rho v)(\gamma_1+\epsilon+\mu+\sigma)}]$$

We now analyze the sensitivity indices of the parameter R_0 and the following results are obtained

For θ

$$\frac{\partial R_0}{\partial\theta}\times(\frac{\theta}{R_0}) = \frac{\omega\alpha_1(T)}{(K)(\gamma_1+\epsilon+\mu+\sigma)}\times\frac{\theta(K)(\gamma_1+\epsilon+\mu+\sigma)}{\omega\theta\alpha_1(T)+\omega\theta_1(1-\rho)v\alpha_1(T)} = \frac{1}{\theta+\theta_1(1-\rho)v}$$

For θ_1

$$\frac{\partial R_0}{\partial \theta_1}\times(\frac{\theta_1}{R_0}) = \frac{\omega(1-\rho)v\alpha_1(T)}{(K)(\gamma_1+\epsilon+\mu+\sigma)}\times\frac{\theta_1(K)(\gamma_1+\epsilon+\mu+\sigma)}{\omega\theta\alpha_1(T)+\omega\theta_1(1-\rho)v\alpha_1(T)} = \frac{\theta_1(1-\rho)v}{\theta+\theta_1(1-\rho)v}$$

For $\alpha_1(T)$

$$\frac{\partial R_0}{\partial \alpha_1(T)}\times(\frac{\alpha_1(T)}{R_0}) = \frac{\omega\theta+\omega\theta_1(1-\rho)v}{(K)(\gamma_1+\epsilon+\mu+\sigma)}\times\frac{\alpha_1(T)(K)(\gamma_1+\epsilon+\mu+\sigma)}{\omega\theta\alpha_1(T)+\omega\theta_1(1-\rho)v\alpha_1(T)} = 1$$

For v

$$\frac{\partial R_0}{\partial v}\times(\frac{v}{R_0}) = \frac{\omega(1-\rho)\theta_1\alpha_1(T)}{(K)(\gamma_1+\epsilon+\mu+\sigma)}\times\frac{v(K)(\gamma_1+\epsilon+\mu+\sigma)}{\omega\theta\alpha_1(T)+\omega\theta_1(1-\rho)v\alpha_1(T)} = \frac{\theta_1(1-\rho)v}{\theta+\theta_1(1-\rho)v}$$

Using parameter values in Table 4.2 the sensitivity indices of R_0 in Table 4.1 are obtained.

These indices measure the relative change in R_0 with respect to the change in the parameters. Therefore, using these indices, we find the parameters that highly affect the R_0 and need to be targeted for intervention strategies.

Table 4.1: Sensitivity indices of R_0 with respect to the model parameter

Parameters	Sensitivity indices
θ	0.159
θ_1	0.044
α_1	1
v	0.044

From Table 4.1 we discuss these parameters and how they affect the R_0 of our $SIRB$ cholera temperature dependent disease transmission model. From the sensitivity indices in Table 4.1, the following can be concluded.

The sensitivity analysis of model (4.1) parameters shows that R_0 is highly sensitive to infection rate of pathogen α_1 that is dependent on temperature.

An increase in infection rate of pathogen α_1 that is dependent on temperature by 10% would increase R_0 by 10% and decreasing it by 10% reduces R_0 by 10%.

Sensitivity analysis also shows that R_0 is also sensitive to the effective contact rate θ on unvaccinated individuals which increases R_0 by 15.9% while the transmission probability for the vaccinated group θ_1 would be much less since if individuals are vaccinated their probability of getting infected would reduce by 4.44%

Through this sensitivity analysis, this study suggest that increasing the temperature of the environment would help reduce the infection rate of the pathogen that depends on temperature since this would help reduce the reproduction number R_0.

4.7 Numerical Simulation

In this section, numerical simulation is performed using the temperature dependent $SIRB$ between-host cholera model to illustrate the theoretical results by numerically solving the model system (4.1). This is done by first taking the initial values from existing literature as shown in $Table$ 4.2. By applying Euler's formulae into the model system (4.1) by letting $n = 1 : T - 1$ yield

$$\begin{aligned}
S_{n+1} &= S_n + dt[(\Lambda_1 - \frac{\omega\theta S_n B_n \alpha_1(T)}{K + B_n} - \frac{\omega\theta_1(1-\rho)vS_n B_n \alpha_1(T)}{K + B_n} - \mu S_n - \rho v S_n] \\
I_{n+1} &= I_n + dt[\frac{\omega\theta S_n B_n \alpha_1(T)}{K + B_n} + \frac{\omega\theta_1(1-\rho)vS_n B_n \alpha_1(T)}{K + B_n} - (\gamma_1 + \epsilon + \mu + \sigma)I_n] \\
R_{n+1} &= R_n + dt[\gamma_1 I_n + \rho v S_n - \mu R_n] \\
B_{n+1} &= B_n + dt[\epsilon I_n - \mu_1 B_n] \qquad (4.14)
\end{aligned}$$

Using the parameter values in table (4.2) and fitting the model system (4.1) in MATLAB software, the results in section (4.7.2) are obtained.

4.7.1 Parameter Values

The parameters values below are described in Table (4.2), these values have been chosen from existing literature and others through estimation.

Table 4.2: Parameter values for the Between-Host Cholera Model

Description	Parameters	Initial value	Source
Susceptible	S	1000	Estimated
Pathogens	B	100000	[42]
Temperature		$T_0 = 23^0C$ and $T = 43^0C$	Estimated
Natural death rate	μ	0.06 day^{-1}	[42]
disease induced death	σ	0.7 day^{-1}	[5]
vaccination rate	v	0.2	[42]
Recovery rate	γ_1	0.1 day^{-1}	[5]
Effective contact rate	θ	0.6 day^{-1}	Estimated
Transmission probability for vaccinated group	θ_1	0.2 day^{-1}	Estimated
Fraction of vaccinated individuals who don't get infected	ρ	0.30 day^{-1}	Estimated
Natural death rate of B	μ_1	0.06 day^{-1}	Estimated

4.7.2 Simulation Results and Discussion

In this section, simulation results are presented using the temperature dependent $SIR - B$ model as described in the *Figures* (4.1), *Figure* (4.2), *Figure* (4.3) and Figure (4.4). The key focus is in Figure (4.2) which shows the behaviour in concentration of *Vibrio cholerae* for different vales of temperature. In relation to a study [34] investigation of water quality in wet and dry seasons under climate change whose result shows that a lot of contaminating materials normally enter the water basin due to the lack of sewage and refinery collection systems that makes waste water of the surrounding villages to flow into water basin. The findings shows that during dry seasons when the temperature is high their is limited supply of clean water for consumption and this contributes to contamination of water bodies through human activities such as poor waste disposal. This implies that during dry season cholera disease will still persist. Relating the results in [34] with our simulation results of the between-host cholera model with temperature dependent parameter, it is observed that when the temperature is high the rate of infection will be low compared to when the temperature is low. This can be seen in Figure (4.1), Figure (4.2), Figure (4.3) and Figure (4.4).

In Figure (4.1), is a graph of B when $T = 43^0C$ and $T = 23^0C$. The concentration of B at $T = 43^0C$ is reduced at a faster rate but when $T = 23^0C$ the population of B is high, this is an indication that vibrios spread and multiply faster at $T = 23^0C$ but they spread and multiply at lower rate when the temperature is high. This is clearly seen in Figure (4.2)

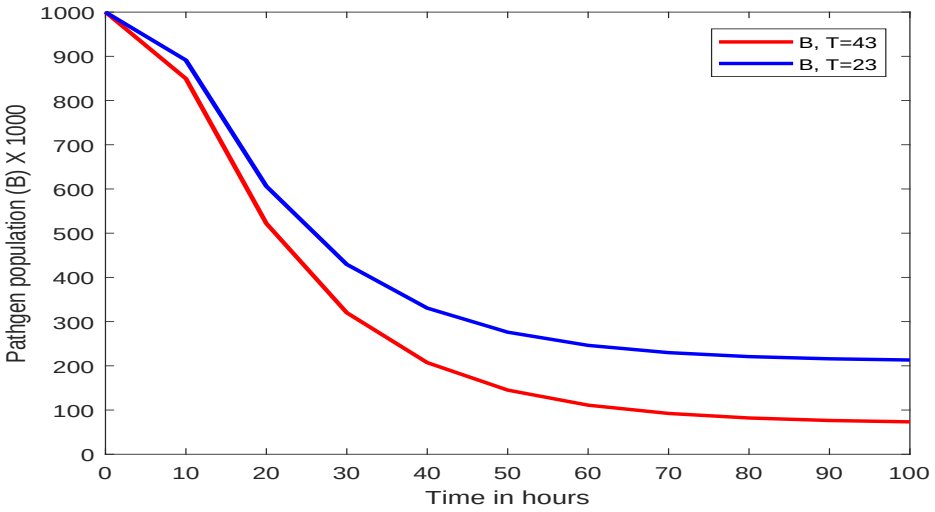

Figure 4.1: Graph of (B) against time for $T = 43^0C$ and $T = 23^0C$

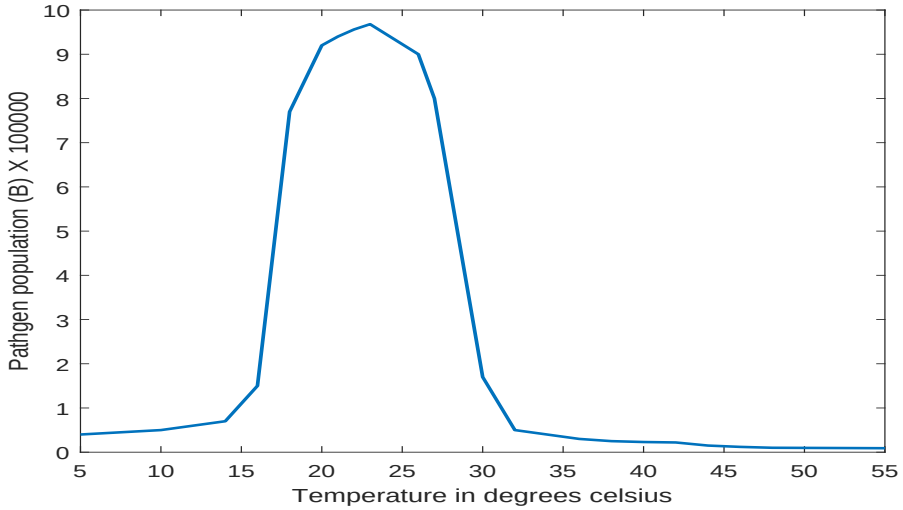

Figure 4.2: Graph of (B) against temperature in degree Celsius

In Figure (4.3), is a graph of susceptible population when $T = 43^0C$, $T = 30^0C$ up-to $T = 23^0C$. The population of susceptible reduces at a faster rate when the temperature is $T = 23^0C$ and at a lower rate when the temperature is high ($T = 43^0C$). This implies that at $T = 23^0C$ there are more pathogens present to cause infection hence more susceptible individuals are being infected .

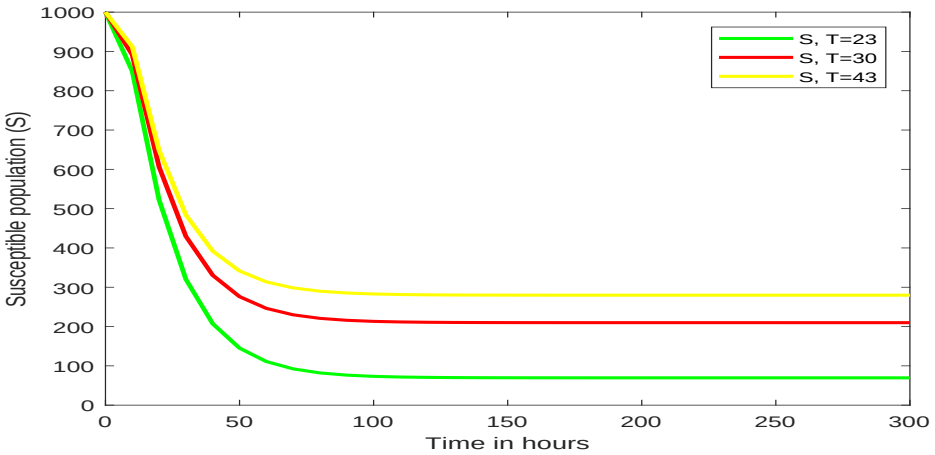

Figure 4.3: Graph of (S) against time when $T = 43^0C$, $T = 30^0C$ and $T = 23^0C$

In Figure (4.4), when $T = 23^0C$ the population of the infected individuals increases at a higher rate compared to when the temperature is $T = 30^0C$ and $T = 43^0C$ respectively. This shows that at $T = 23^0C$ there are more pathogens active to cause infections which leads to many individuals being infected, after sometimes this population decreases. Despite the differences in temperature, there will still be infected individuals which shows persistence in cholera disease.

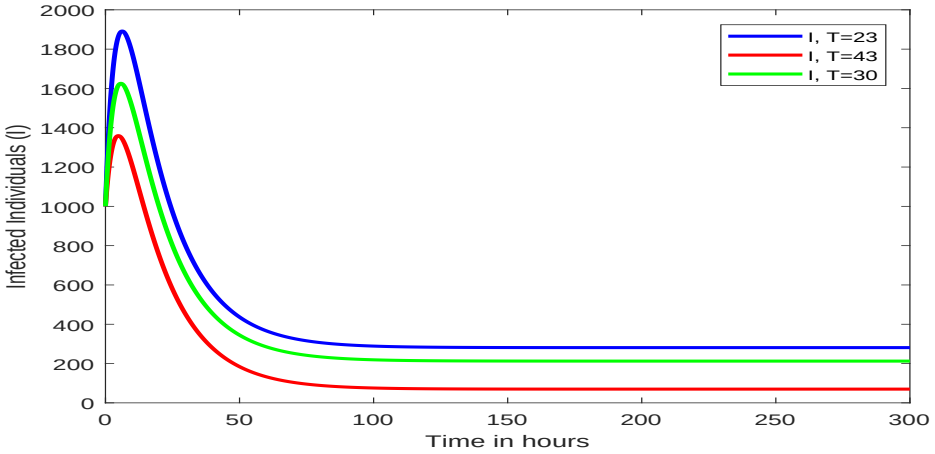

Figure 4.4: Graph of I against time when $T = 43^0C$ and $T = 23^0C$

4.8 Conclusion

A between-host cholera model with temperature dependent parameter has been formulated. The DFE points of the model is locally and globally asymptotically stable when $R_0 < 1$, this implies that there is extinction of the pathogen in an individual. On the other hand, when $R_0 > 1$, the DFE becomes unstable. The model also has endemic equilibrium point which is locally asymptotically stable when $R_0 > 1$, this means that there is persistent infection. Numerical analysis has been performed to graphically illustrate the solutions to the model's analytic solutions and simulation result shows that *Vibrio cholerae* pathogens can multiply and spread faster at temperatures of 23^0C but between $23^0C < T \leq 43^0C$ their multiplication is hindered hence at temperatures 23^0C, there will be more pathogens active to cause infection compared to when the temperature is high. Sensitivity analysis of model (4.1) parameters is done and shows that infection rate of pathogen α_1 that is dependent on temperature would reduce R_0 by 10%, also the effective contact rate θ for unvaccinated individuals will increase R_0 by 15.9% while the transmission probability for the vaccinated group θ_1 would be much less if individuals are vaccinated, this would reduce R_0 by 4.44% . Through sensitivity analysis, this study suggest that increasing the temperature of the food/water before consumption through heating would help reduce the infection rate of the pathogen that depends on temperature since this would help reduce the reproduction number R_0 of the pathogen.

CHAPTER FIVE

DYNAMICS OF THE FRACTIONAL ORDER BETWEEN-HOST CHOLERA MODEL WITH TEMPERATURE DEPENDENT PARAMETER

5.1 Introduction

In this chapter a between host mathematical cholera model (4.1) is expressed in Caputo fractional order derivative form and then analysed. Mathematical models developed in fractional order are useful than the ordinary order model as it can be used in predicting outbreaks of infectious diseases. For instance, Sani and Mohammed [35] developed a Caputo sense fractional order derivative model and analysed its dynamics with control measures i.e treatment, hygiene consciousness and vaccine. The result show that lower fractional order values gives lower values of susceptible but gives higher number of infected individuals as shown in *Figure* 5.1 and *Figure* 5.3. The findings of the study further shows that the fractional order results gave a better, efficient and portrays a successful useable controls due its memory effect [24].

Fractional order derivative models are also useful in giving information about the memory that can describe the model in real cases. Therefore, this study adopts the use of Caputo fractional order time derivative to analyse the dynamics of between-host cholera model (4.1) and compare its results with that obtained from the analysis of ordinary derivatives between host cholera model in chapter (4). The existence and uniqueness of the solution has been determined using Banach fixed point analysis. Stability analysis of DFE and EE has been done in chapter (4) which shows that its solutions are stable. In section (5.5), iterative solutions

of the model has been done and the results show that the between-host Caputo derivative cholera model is stable. Finally, graphical results for the model has been done using Matlab software to show the effect of some sensitive parameters for possible minimization of cholera infection in the population. Numerical analysis of the Caputo fractional order derivative also show that cholera disease outbreaks mostly occurs when there is low temperature of the environment.

5.2 Basic Fractional Model Description

In this section brief definitions regarding fractional derivative is given. These definitions are applied to the analysis of the model.

Definition 5.2.1. *Consider $X \in C^n$ be a function, then the well known classical derivative with fractional order α in $(n-1, n)$ where $n \in N$ [24] is defined as*

$${}^{C}D_t^{\alpha} = \frac{1}{\Gamma(n-\alpha)} \int_0^t x^n(\rho)(t-\rho)^{n-\alpha-1} d\rho \text{ Where } {}^{C}D_t^{\alpha}(x(t)) \to x^{'}(t) as \alpha \to t$$

Definition 5.2.2. *Let x^* denote the equilibrium point of the Caputo fractional model then;*

$${}^{C}D_t^{\alpha}(x(t)) = h(t, x(t)), \alpha \in (0,1) iff h(t, x^*) = 0$$

Definition 5.2.3. *The corresponding integral with fractional order $\alpha > 0$ of the function $x : \mathbb{R}^+ \to \mathbb{R}$ is described as; $I_t^{\alpha} = \frac{1}{\Gamma(x)} \int_0^t x(\rho)(t-\rho)^{\alpha-1} d\rho, 0 < \alpha < 1, t > 0$*

Definition 5.2.4. *A function $f(t, y)$ satisfy a Lipschitz condition in the variable y on a set $D \in \mathbb{R}^2$ if a constant $L > 0$ exists with $|f(t, y_1) - f(t, y_2)| \leq L|y_1 - y_2|$ whenever (t, y_1) and (t, y_2) are in D.*

From the model described in chapter (4), the representation of the cholera model in terms of fractional differential equation is given by;

$$
\begin{aligned}
{}^{C}D^{\alpha}_{0,t}(S(t)) &= \frac{1}{\Gamma(1-\alpha)}\int_0^t (t-\rho)^{-\alpha} S^{'}(\rho)d\rho \\
{}^{C}D^{\alpha}_{0,t}(I(t)) &= \frac{1}{\Gamma(1-\alpha)}\int_0^t (t-\rho)^{-\alpha} I^{'}(\rho)d\rho \\
{}^{C}D^{\alpha}_{0,t}(R(t)) &= \frac{1}{\Gamma(1-\alpha)}\int_0^t (t-\rho)^{-\alpha} R^{'}(\rho)d\rho \\
{}^{C}D^{\alpha}_{0,t}(B(t)) &= \frac{1}{\Gamma(1-\alpha)}\int_0^t (t-\rho)^{-\alpha} B^{'}(\rho)d\rho
\end{aligned} \tag{5.1}
$$

Therefore the cholera model in Caputo operator form is given by;

$$
\begin{aligned}
{}^{C}D^{\alpha}_{0,t}(S(t)) &= \Lambda_1 - \frac{\omega\theta SB\alpha_1(T)}{K+B} - \frac{\omega\theta_1(1-\rho)vSB\alpha_1(T)}{K+B} - \mu S - \rho vS \\
{}^{C}D^{\alpha}_{0,t}(I(t)) &= \frac{\omega\theta SB\alpha_1(T)}{K+B} + \frac{\omega\theta_1(1-\rho)vSB\alpha_1(T)}{K+B} - (\gamma_1 + \epsilon + \mu + \sigma)I \\
{}^{C}D^{\alpha}_{0,t}(R(t)) &= \gamma_1 I + \rho vS - \mu R \\
{}^{C}D^{\alpha}_{0,t}(B(t)) &= \epsilon I - \mu_1 B
\end{aligned} \tag{5.2}
$$

5.3 Positivity of the Model

Model (5.2) describes human population whose values will never be negative. We therefore assume that all variables and parameters are non-negative for all time, $t \geq 0$. Thus solutions of model (5.2) are positive.

5.4 Existence and Uniqueness of the Model Solutions

In this section, existence and uniqueness of solutions for the Caputo operator is explored with the help of fixed point theory. Let $Q(G)$ denote a Banach space consisting of real valued functions over the interval G=[0,a] with norm defined by;

$$\|S\| = sup_{t\in G}\|S(t)\|$$

$$\|I\| = sup_{t\in G}\|I(t)\|$$

$$\|R\| = sup_{t\in G}\|R(t)\|$$

$$\|B\| = sup_{t\in G}\|B(t)\|$$

This norm is given by $\|(S, I, R, B)\| = \|S\| + \|I\| + \|R\| + \|B\|$

Proof. Using Caputo integral, model (5.2) is written in the form

$$\begin{aligned}
S(t) &= S(0) +^C I^{\alpha}_{0,t}\{\Lambda_1 - \frac{\omega\theta SB\alpha_1(T)}{K+B} - \frac{\omega\theta_1(1-\rho)vSB\alpha_1(T)}{K+B} - \mu S - \rho vS\}\\
I(t) &= I(0) +^C I^{\alpha}_{0,t}\{\frac{\omega\theta SB\alpha_1(T)}{K+B} + \frac{\omega\theta_1(1-\rho)vSB\alpha_1(T)}{K+B} - (\gamma_1 + \epsilon + \mu + \sigma)I\}\\
R(t) &= R(0) +^C I^{\alpha}_{0,t}\{\gamma_1 I + \rho vS - \mu R\}\\
B(t) &= B(0) +^C I^{\alpha}_{0,t}\{\epsilon I - \mu_1 B\} \qquad (5.3)
\end{aligned}$$

From $Definition$ 5.2.3

$$\begin{aligned}
S(t) &= S(0) + \frac{1}{\Gamma(\alpha)}\int_0^t (t-G)^{\alpha-1}k_1(G, S(G))dG\\
I(t) &= I(0) + \frac{1}{\Gamma(\alpha)}\int_0^t (t-G)^{\alpha-1}k_2(G, I(G))dG\\
R(t) &= R(0) + \frac{1}{\Gamma(\alpha)}\int_0^t (t-G)^{\alpha-1}k_3(G, R(G))dG\\
B(t) &= B(0) + \frac{1}{\Gamma(\alpha)}\int_0^t (t-G)^{\alpha-1}k_4(G, B(G))dG \qquad (5.4)
\end{aligned}$$

The constants k_1, k_2, k_3 and k_4 are;

$$\begin{aligned}
k_1(t, S(t)) &= \Lambda_1 - \frac{\omega\theta SB\alpha_1(T)}{K+B} - \frac{\omega\theta_1(1-\rho)vSB\alpha_1(T)}{K+B} - \mu S - \rho vS\\
k_2(t, I(t)) &= \frac{\omega\theta SB\alpha_1(T)}{K+B} + \frac{\omega\theta_1(1-\rho)vSB\alpha_1(T)}{K+B} - (\gamma_1 + \epsilon + \mu + \sigma)I\\
k_3(t, R(t)) &= \gamma_1 I + \rho vS - \mu R\\
k_4(t, B(t)) &= \epsilon I - \mu_1 B \qquad (5.5)
\end{aligned}$$

The expressions $k_1(t, S(t))$, $k_2(t, I(t))$, $k_3(t, R(t))$ and $k_4(t, B(t))$ satisfy the *Lipchitz* conditions with $S(t)$, $I(t)$, $R(t)$ and $B(t)$ having an upper bound. Putting the functions $S(t)$ and $S^*(t)$ into consideration and using similar approach for the remaining equations yields;

$$\|k_1(t, S(t)) - k_1(t, S^*(t))\| = \|\Lambda_1 - \frac{\omega\theta SB\alpha_1(T)}{K+B} - \frac{\omega\theta_1(1-\rho)vSB\alpha_1(T)}{K+B}\| -$$
$$\|\mu S(t) - \rho v S(t) - S^*(t))\|$$

Let $l_1 = \|\Lambda_1 - \frac{\omega\theta SB\alpha_1(T)}{K+B} - \frac{\omega\theta_1(1-\rho)vSB\alpha_1(T)}{K+B} - \mu S - \rho vS\|$

Using the same approach for the remaining equations yields;

$$\|k_1(t, S(t)) - k_1(t, S^*(t))\| \leq l_1\|(S(t) - S^*(t))\|$$

$$\|k_2(t, I(t)) - k_2(t, I^*(t))\| \leq l_2\|(I(t) - I^*(t))\|$$

$$\|k_3(t, R(t)) - k_3(t, R^*(t))\| \leq l_3\|(R(t) - R^*(t))\|$$

$$\|k_4(t, B(t)) - k_4(t, B^*(t))\| \leq l_4\|(B(t) - B^*(t))\|$$

Hence the Lipchitz condition is satisfied. The equations in (5.5) can also be shown recursively as;

$$\begin{aligned}
S_n(t) &= S(0) + \frac{1}{\Gamma(\alpha)}\int_0^t (t-G)^{\alpha-1}k_1(G, S_{n-1}(G))dG \\
I_n(t) &= I(0) + \frac{1}{\Gamma(\alpha)}\int_0^t (t-G)^{\alpha-1}k_2(G, I_{n-1}(G))dG \\
R_n(t) &= R(0) + \frac{1}{\Gamma(\alpha)}\int_0^t (t-G)^{\alpha-1}k_3(G, R_{n-1}(G))dG \\
B_n(t) &= B(0) + \frac{1}{\Gamma(\alpha)}\int_0^t (t-G)^{\alpha-1}k_4(G, B_{n-1}(G))dG
\end{aligned} \tag{5.6}$$

Therefore the corresponding differences among the successive terms along with the initial conditions of the model takes the form

$$\begin{aligned}
\Phi S_{1n}(t) &= S_n(t) - S_{n-1}(t) = \frac{1}{\Gamma(\alpha)} \int_0^t (t-G)^{\alpha-1} \{k_1(G, S_{n-1}(G)) - k_1(G, S_{n-2}(G))\} dG \\
\Phi I_{1n}(t) &= I_n(t) - I_{n-1}(t) = \frac{1}{\Gamma(\alpha)} \int_0^t (t-G)^{\alpha-1} \{k_1(G, I_{n-1}(G)) - k_1(G, I_{n-2}(G))\} dG \\
\Phi R_{1n}(t) &= R_n(t) - R_{n-1}(t) = \frac{1}{\Gamma(\alpha)} \int_0^t (t-G)^{\alpha-1} \{k_1(G, R_{n-1}(G)) - k_1(G, R_{n-2}(G))\} dG \\
\Phi B_{1n}(t) &= B_n(t) - B_{n-1}(t) = \frac{1}{\Gamma(\alpha)} \int_0^t (t-G)^{\alpha-1} \{k_1(G, B_{n-1}(G)) - k_1(G, B_{n-2}(G))\} dG
\end{aligned} \tag{5.7}$$

From the above equation it is noted that; $S_n(t) = \sum_{j=0}^{n} \Phi S_{1j}(t)$, $I_n(t) = \sum_{j=0}^{n} \Phi I_{1j}(t)$, $R_n(t) = \sum_{j=0}^{n} \Phi R_{1j}(t)$ and $B_n(t) = \sum_{j=0}^{n} \Phi B_{1j}(t)$.

It can now be considered that

$$\Phi S_{1,n-1}(t) = S_{n-1}(t) - S_{n-2}(t)$$

$$\Phi I_{1,n-1}(t) = I_{n-1}(t) - I_{n-2}(t)$$

$$\Phi R_{1,n-1}(t) = R_{n-1}(t) - R_{n-2}(t)$$

$$\Phi B_{1,n-1}(t) = B_{n-1}(t) - B_{n-2}(t)$$

Therefore the following are obtained from the above

$$\begin{aligned}
\|\Phi S_{1n}(t)\| &\leq \frac{1}{\Gamma(\alpha)} l_1 \int_0^t (t-G)^{\alpha-1} \|\Phi S_{n-1}(G)\| dG \\
\|\Phi I_{1n}(t)\| &\leq \frac{1}{\Gamma(\alpha)} l_2 \int_0^t (t-G)^{\alpha-1} \|\Phi I_{n-1}(G)\| dG \\
\|\Phi R_{1n}(t)\| &\leq \frac{1}{\Gamma(\alpha)} l_3 \int_0^t (t-G)^{\alpha-1} \|\Phi R_{n-1}(G)\| dG \\
\|\Phi B_{1n}(t)\| &\leq \frac{1}{\Gamma(\alpha)} l_4 \int_0^t (t-G)^{\alpha-1} \|\Phi B_{n-1}(G)\| dG
\end{aligned} \tag{5.8}$$

Hence $S(t)$, $I(t)$, $R(t)$ and $B(t)$ describe the bounded functions and the expressions k_1, k_2, k_3 and k_4 satisfy the *Lipchitz* condition. □

Theorem 5.4.1. *The Caputo cholera epidemic model has a unique solution for* $t \in [0, a]$ *if* $\frac{1}{\Gamma(\alpha)} l_j m < 1$, *j=1,....4.*

Proof. Since $S(t)$, $I(t)$, $R(t)$ and $B(t)$ are bounded and expressions k_1, k_2, k_3 and k_4 satisfy the *Lipchitz* condition. By recursive principle, the above equations (5.8) implies that;

$$\begin{aligned}
\|\Phi S_{1n}(t)\| &\leq \|S_0(t)\|(\frac{m}{\Gamma(\alpha)} l_1)^n \\
\|\Phi I_{1n}(t)\| &\leq \|I_0(t)\|(\frac{m}{\Gamma(\alpha)} l_2)^n \\
\|\Phi R_{1n}(t)\| &\leq \|R_0(t)\|(\frac{m}{\Gamma(\alpha)} l_3)^n \\
\|\Phi B_{1n}(t)\| &\leq \|B_0(t)\|(\frac{m}{\Gamma(\alpha)} l_4)^n
\end{aligned} \tag{5.9}$$

Therefore the sequence (5.9) exists and obey the conditions described below; $\|\Phi S_{1n}(t)\| \to 0$, $\|\Phi I_{1n}(t)\| \to 0$, $\|\Phi R_{1n}(t)\| \to 0$, and $\|\Phi B_{1n}(t)\| \to 0$ as $n \to \infty$ Therefore

$$\|S_{n+l}(t) - S_n(t)\| \leq \sum_{j=n+1}^{n+l} X_i^j = \frac{X_1^{n+1} - X_1^{n+l+1}}{1 - X_1}$$

$$\|I_{n+l}(t) - I_n(t)\| \leq \sum_{j=n+1}^{n+l} X_i^j = \frac{X_1^{n+1} - X_2^{n+l+1}}{1 - X_2}$$

$$\|R_{n+l}(t) - R_n(t)\| \leq \sum_{j=n+1}^{n+l} X_i^j = \frac{X_1^{n+1} - X_3^{n+l+1}}{1 - X_3}$$

$$\|B_{n+l}(t) - B_n(t)\| \leq \sum_{j=n+1}^{n+l} X_i^j = \frac{X_1^{n+1} - X_4^{n+l+1}}{1 - X_4}$$

Therefore using the hypothesis $\frac{1}{\Gamma(\alpha)} l_j m < 1$ and S_n, I_n, R_n and B_n is the Cauchy sequence and it implies that the fractional order cholera Caputo derivative has a unique solution. Hence completes the proof for the desired results for the fractional order model (5.2). □

5.5 Iterative Solutions and Stability Analysis

In this section, the analysis of model (5.2) is performed to establish if the Caputo-fractional between-host cholera model is stable.

Theorem 5.5.1. *Let $(B, \|.\|)$ denote a Banach space and G^* define a self map on B. Further, $Z_{n+1} = h(G^*, Z_n)$ shows the recursive expression while $C(G^*)$ denote the fixed point set upon G^*. Also by definition $\|x^*_{n+1} - h(G^*, x^*_n)\|$ such that $\{x^*_n \in B\}$. Then the iterative approach $x_{n+1} = h(G^*, y_n)$, G^* is stable if $\lim_{n\to\infty} c_n = 0$ for $z_{n+1} = G^*$ where n is taken as the picards iteration then G^* iteration is stable.*

The above theorem is summarised as follows; $(B, \|.\|)$ define a Banach space and G^* is a self map upon B, then for all $x, y \in B$ yield;

$$\begin{aligned}
S_{n+1}(t) &= S_n(t) + L^{-1}\{\frac{1}{S^\alpha}L[\Lambda_1 - \frac{\omega\theta SB\alpha_1(T)}{K+B} - \frac{\omega\theta_1(1-\rho)vSB\alpha_1(T)}{K+B} - \mu S - \rho vS]\} \\
I_{n+1}(t) &= I_n(t) + L^{-1}\{\frac{\omega\theta SB\alpha_1(T)}{K+B} + \frac{\omega\theta_1(1-\rho)vSB\alpha_1(T)}{K+B} - (\gamma_1 + \epsilon + \mu + \sigma)I]\} \\
R_{n+1}(t) &= R_n(t) + L^{-1}\{\frac{1}{S^\alpha}L[\gamma_1 I + \rho vS - \mu R]\} \\
B_{n+1}(t) &= B_n(t) + L^{-1}\{\frac{1}{S^\alpha}L[\epsilon I - \mu_1 B]\} \qquad (5.10)
\end{aligned}$$

Let P define a self map then

$$P(S_n(t)) = S_{n+1}(t)$$

=

$$S_n(t) + L^{-1}\{\frac{1}{S^\alpha}L[\{\Lambda_1 - \frac{\omega\theta SB\alpha_1(T)}{K+B} - \frac{\omega\theta_1(1-\rho)vSB\alpha_1(T)}{K+B} - \mu S - \rho vS]\}$$

$$P(I_n(t)) = I_{n+1}(t)$$

=

$$I_n(t) + L^{-1}\{\frac{1}{S^\alpha}L[\frac{\omega\theta SB\alpha_1(T)}{K+B} + \frac{\omega\theta_1(1-\rho)vSB\alpha_1(T)}{K+B} - (\gamma_1 + \epsilon + \mu + \sigma)I]\}$$

$$P(R_n(t)) = R_{n+1}(t) = R_n(t) + L^{-1}\{\frac{1}{S^\alpha}L[\gamma_1 I + \rho v S - \mu R]\}$$

$$P(B_n(t)) = B_{n+1}(t) = B_n(t) + L^{-1}\{\frac{1}{S^\alpha}L[\epsilon I - \mu_1 B]\}$$

Therefore P is stable if the following conditions are satisfied;

$$1 - [(1 - \Lambda_1 f_1 - \frac{\omega\theta\alpha_1(T)}{K}f_2 - \frac{\omega\theta_1(1-\rho)v\alpha_1(T)}{K}f_3 - (\rho v + \mu)k_1]] < 1$$

$$1 - [\frac{\omega\theta\alpha_1(T)}{K}f_4 + \frac{\omega\theta_1(1-\rho)v\alpha_1(T)}{K}f_5 - (\gamma_1 + \epsilon + \mu + \sigma)k_2] < 1$$

$$1 - [\gamma_1 + \rho v - \mu]k_3 < 1$$

$$1 - [\epsilon - \mu_1]k_4 < 1$$

Proof. Since the map P is a fixed point, taking the norm of the following

$$\|L^{-1}\{\frac{1}{S^\alpha}L[\Lambda - \frac{\omega\theta S_n B_n\alpha_1(T)}{K + B_n} - \frac{\omega\theta_1(1-\rho)vS_nB_n\alpha_1(T)}{K+B_n} - \rho v S_n - \mu S_n]\}\| -$$

$$\|L^{-1}\{\frac{1}{S^\alpha}L[\Lambda_1 - \frac{\omega\theta S_m B_m\alpha_1(T)}{K + B_m} - \frac{\omega\theta_1(1-\rho)vS_mB_m\alpha_1(T)}{K+B_m} - \rho v S_m - \mu S_m]\}$$

$$+(S_n(t) - (S_m(t))\|$$

This implies that;

$$\|P[(S_n(t))] - P[(S_m(t))]\| \leq \|(S_n(t) - (S_m(t))\| + L^{-1}\{\frac{1}{S^\alpha}\|S_n(I_n - I_m)\| +$$

$$\|I_n(S_n - S_m)\| + \|B_n(S_n - S_m)\|\}$$

From the above it follows that;

$$\|(I_n(t) - I_m(t)\| \cong \|(S_n(t) - S_m(t)\|$$

$$\|(R_n(t) - R_m(t)\| \cong \|(S_n(t) - S_m(t)\|$$

$$\|(B_n(t) - B_m(t)\| \cong \|(S_n(t) - S_m(t)\|$$

Hence the sequence $S_n(t)$, $I_m(t)$, $R_n(t)$ and $B_m(t)$ are convergent and bounded. Therefore for $n = 1, 2....4$, $S > 0$ for all t we have ;

$$\|P[(S_n(t))] - P[(S_m(t))]\| \leq \{1 - [\Lambda_1 f_1 - \frac{\omega\theta\alpha_1(T)}{K} f_2 - \frac{\omega\theta_1(1-\rho)v\alpha_1(T)}{K} f_3$$

$$-(\rho v + \mu)k_1]\}\|(S_n(t) - S_m(t)\|$$

$$\|P[(I_n(t))] - P[(I_m(t))]\| \leq \{1 - [\frac{\omega\theta\alpha_1(T)}{K} f_4 + \frac{\omega\theta_1(1-\rho)v\alpha_1(T)}{K} f_5$$

$$-(\gamma_1 + \epsilon + \mu + \sigma)k_2]\}\|(I_n(t) - I_m(t)\|$$

$$\|P[(R_n(t))] - P[(R_m(t))]\| \leq \{1 - [\gamma - \mu]k_3\}\|(R_n(t) - R_m(t)\|$$

$$\|P[(B_n(t))] - P[(B_m(t))]\| \leq \{1 - [\epsilon - \mu_1]k_4\}\|(B_n(t) - B_m(t)\|$$

This completes the proof and it shows that G^* iteration is stable. Hence implying that the between host caputo derivative cholera model is stable.

□

5.6 Numerical Simulation

In this section, simulation results and discussion of the Caputo-cholera between host model is presented. The model (5.2) is simulated for different parameter values of the order of fractional derivative $\alpha \in [0, 1]$. The numerical analysis done based on the iterative solution of the model in order to help in determining the impact of control measures and sensitive parameters that can help reduce cholera disease. By fitting the iterative solution of the model (5.2) in MATLAB software,

simulation results in section (5.6.2) is obtained. This is done using the biological parameter values from existing literature as in Table (5.1).

$$
\begin{aligned}
S_{n+1}(t) &= S_n(t) + L^{-1}\{\frac{1}{S^\alpha}L[\frac{\omega\theta SB\alpha_1(T)}{K+B} - \frac{\omega\theta_1(1-\rho)vSB\alpha_1(T)}{K+B} - \mu S - \rho vS]\} \\
I_{n+1}(t) &= I_n(t) + L^{-1}\{\frac{1}{S^\alpha}L[\frac{\omega\theta SB\alpha_1(T)}{K+B} + \frac{\omega\theta_1(1-\rho)vSB\alpha_1(T)}{K+B} - (\gamma_1+\epsilon+\mu+\sigma)I]\} \\
R_{n+1}(t) &= R_n(t) + L^{-1}\{\frac{1}{S^\alpha}L[\gamma_1 I + \rho vS - \mu R]\} \\
B_{n+1}(t) &= B_n(t) + L^{-1}\{\frac{1}{S^\alpha}L[\epsilon I - \mu_1 B]\} \qquad (5.11)
\end{aligned}
$$

5.6.1 Parameter Values

The parameters values below have been obtained from existing literature and others estimated.

Table 5.1: Parameter values for the Fractional order Between-Host Cholera Model

Description	Parameters	Initial value	Source
Susceptible	S	2000	Estimated
Temperature	T	$0 < T_0 \leq 23^0C$ *and* $23^0C < T \leq 43^0C$	Estimated
Natural death rate	μ	0.06 day^{-1}	[5]
disease induced death	σ	0.7 day^{-1}	[5]
vaccine	v	0.2	[5]
Recovery rate	γ_1	0.1 day^{-1}	[5]
Recruitment rate of S	Λ_1	0.02 day^{-1}	Estimated
Caputo operator	α	$0 \leq \alpha \leq 1$	Estimated
Natural death rate of B	μ_1	0.06 day^{-1}	Estimated
Effective contact rate	θ	0.6 day^{-1}	Estimated
Transmission probability for vaccinated group	θ_1	0.2 day^{-1}	Estimated
Fraction of vaccinated individuals who don't get infected	ρ	0.30 day^{-1}	Estimated

5.6.2 Simulation Results and Discussion

The figures 5.1, 5.2 and 5.3 describes the model's different solutions illustrated graphically for different values of α. From Figure (5.1) it can be seen that healthy individuals increases with decreases in the caputo operator α. The results show that healthy individuals increases with decreases in the caputo operator α in the range 0.4 to 0.7 as temperature increases in the range $T = 23^0C$ to $T = 43^0C$.

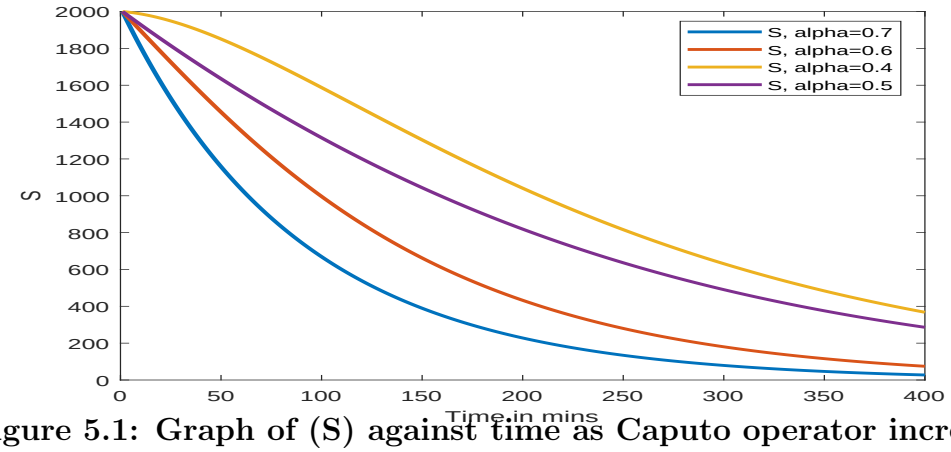

Figure 5.1: Graph of (S) against time as Caputo operator increases.

For recovered individuals the population increases as α increases as shown in Figure (5.2)

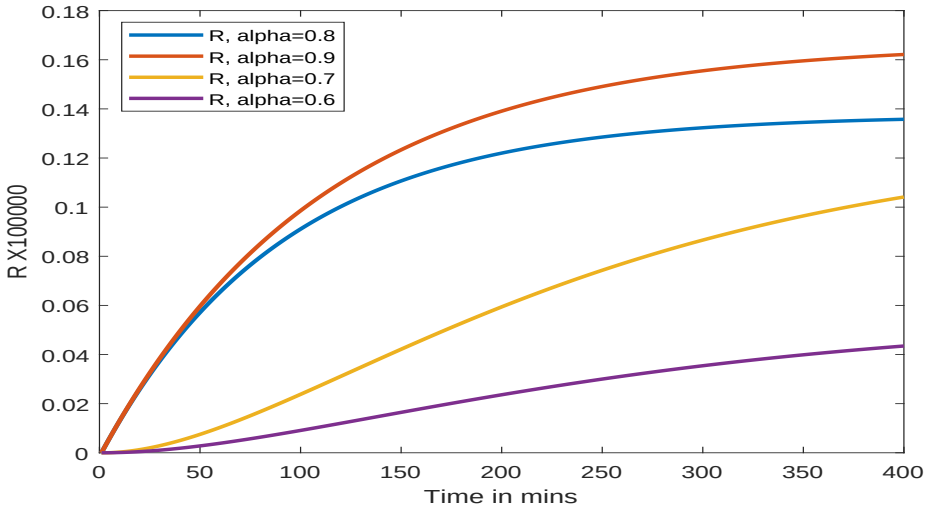

Figure 5.2: Graph of (R) against time as Caputo operator increases.

The impact of effective contact rate θ is shown in Figure (5.3). It is observed that this parameter is reduced when $23^0C < T \leq 43^0C$, thus significance decrease in cases of infection as Caputo operator α decreases. When $\alpha = 0.9$, $T = 23^0C$, $\alpha = 0.7$, $T = 28^0C$, $\alpha = 0.6$, $T = 35^0C$ and $\alpha = 0.4$, $T = 43^0C$,This shows that cholera incidence can be reduced if the environmental temperature is varied in the interval $23^0C < T \leq 43^0C$ and through this the environmental vibrios are reduced.

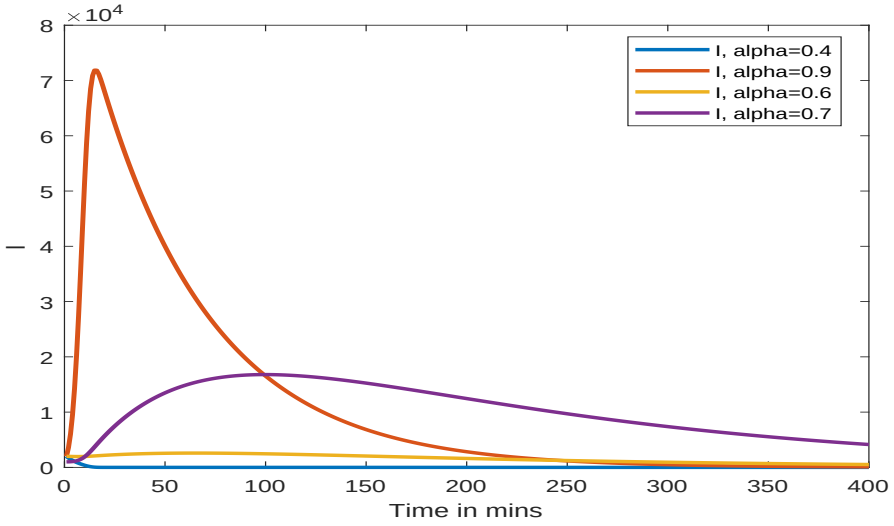

Figure 5.3: Graph of (I) against time as Caputo operator increases with $23^0C < T \leq 43^0C$.

5.7 Conclusion

A fractional order cholera model has been presented, the existence and uniqueness of solutions of the model has been done with the help of fixed point theory and the results shows that $S(t)$, $I(t)$, $R(t)$ and $B(t)$ describe the bounded functions. Iterative solution of the model show that its solution are stable. Numerical solution of the model shows that population of healthy individuals will increase as Caputo operator α decreases. Also as the contact rate increases when $\alpha_1(T)$ is in the range $23^0C < T \leq 43^0C$ then there will be significance decrease in cholera disease, this reduces the environmental vibrios.

CHAPTER SIX

CONCLUSION AND RECOMMENDATION

6.1 Introduction

In this chapter, the conclusion of this study is presented. This will enable us to draw recommendations of the study. We therefore make conclusions and recommendations in section (6.2) and (6.3) respectively, the recommendations are in line with the results of the study as in Chapter 3, Chapter 4 and Chapter 5 respectively.

6.2 Conclusion

This study focused on developing both within-host and between-host cholera model. The main focus was to investigate the impact of vaccination on the dynamics of in-host cholera infection. The findings shows that if vaccine efficacy γ is high then the rate of infection of cells will be low. The IFE point of the models are both locally and globally asymptotically stable. IE point is also locally asymptotically stable when $R_0 > 1$. Numerical analysis shows that when the vaccine efficacy is high, there will be low infection of cells. Numerical simulation of the between-host model 4.1 shows that *Vibrio cholerae* pathogens can spread and multiply faster under low temperatures of $T \leq 23^0C$ but between $23^0C < T \leq 43^0C$ their multiplication and spread is hindered, which implies that they can cause infection at a higher rate when the temperature is low but at high temperature cholera infection is reduced. Sensitivity shows that an increase in infection rate of pathogen α_1 that is dependent on temperature by 10% would increase R_0 by 10% and decreasing it by 10% reduces R_0 by 10%. It further shows that the effective contact rate θ on unvaccinated individuals will increase R_0 by 15.9% while the transmission probability for the vaccinated group θ_1 would be much less since if individuals are

vaccinated their probability of getting infected would reduce by 4.44%. Therefore increasing the temperature of the environment would help reduce the infection rate of the pathogen that depends on temperature since this would help reduce the reproduction number, R_0. A fractional order cholera model has been presented in Chapter 5, the existence and uniqueness of solutions of the model has been done with the help of fixed point theory and the results shows that the solutions are bounded. Iterative solution of the model show that the solution of the model is stable which conforms to the analysis done in Chapter 4. Numerical solution of the model shows that population of healthy individuals will increase as Caputo operator α decreases. Also as the contact rate increases when $\alpha_1(T)$ is in the range $23^0C < T \leq 43^0C$ then there will be significance decrease in infection since there will be reduction in environmental vibrios. Finally the numerical simulation of the Caputo fractional order derivative shows that cholera disease outbreaks mostly occurs when there is low temperature of the environment hence useful in predicting cholera outbreaks.

6.3 Recommendations

Since in our model analysis we observed that when vaccine efficacy is high the number of cells getting infected reduces, and the lower the temperature of the environment the higher the rate of infection, The study, therefore, recommends that human population in cholera endemic areas should be vaccinated against cholera before any outbreak occurs. This could help reduce the burden of cholera disease when there is an outbreak. Secondly, since increasing the temperature of food/water before consumption reduces the infection rate of pathogens, the study therefore recommends that the public should be made aware that heating food before consumption should be mandatory.

REFERENCES

[1] A. I. Dell, S. Pawar, and V. M. Savage (2011). Systematic variation in the temperature dependence of physiological and ecological traits, *Proc. Nat. Acad. Sci. USA,* **108(26)**, 10591–10596.

[2] Arino J., Mc Cluskey, C.C and Van Den Driessche, P. (2003). Global resulst for an epidemic model with vaccination that exhibits backward bifurcation *Journal on Applied Mathematics*, **64**, 260-276.

[3] Alexander, M.E. *et al* .(2004). A vaccination model for transmission dynamics of influenza. *Journal on Applied Dynamical Systems* **3**, 503-524.

[4] Abdon Atangana and Dumitru Baleanu. (2016). New fractional derivatives with nonlocal and non-singular kernel: Theory and application to heat transfer model. *arXiv preprint arXiv*: 1602.03408.

[5] Center for Health Protection.(2011). Epidemiology, prevention and control of cholera in Hong Kong, *CHC*, 4-5.

[6] Christaki, Eirini, Panagiotis Dimitriou, Katerina Pantavou, and Georgios K. Nikolopoulos. (2020). The Impact of Climate Change on Cholera: A Review on the Global Status and Future Challenges. *Atmosphere* **1**1(5) 449.

[7] Chayu Yang, Feng Bao and Jin Wang. (2018). A multi-scale cholera model linking between-host and within-host dynamics, *International Journal of Biomathematics* **11(3)**, 1-23.

[8] Cholera vaccines. (2010). WHO position paper. *Weekly Epidemiol Rec*, **8**5(13), 117-128.

[9] Cai L.M, and Song, X. Global analysis of an epidemic model with vaccination. (2018). *Journal of Applied Mathematics and Computing*,**57**, 605-628.

[10] Castillo-Chavez, C., Song, B.J. (2004). Dynamical models of tuberculosis and their applications, *Math. Biosci. Eng.***1**, 361–404

[11] Castillo-Chavez, Z. Feng, and W. Huang. (2002). On the computation of R_0 and its role on global stability, in Mathematical Approaches for Emerging and Reemerging Infectious Diseases, *Eds.Springer,NewYork, NY, USA,* **125**, 229 – 250.

[12] Conrad Ratchford and Jin Wang. (2019). Modeling cholera dynamics at multiple scales: environmental evolution, between-host transmission, and within-host interaction, *Mathematical Biosciences and Engineering,* **16(2)**: 782-812.

[13] Driessche, P. V. and Watmough, J. (2002). Reproduction numbers and subthreshold endemic equilibria for compartmental models of disease transmission, *Mathematical Biosciences,* 180(2), 29–48.

[14] Eunice E. Ukwajunor, Eno E. E. Akarawak and Israel Olutunji Abiala. (2002). Mathematical modeling of the impact of temperature variations and immigration on malaria prevalence in Nigeria, *International Journal of Biomathematics*,**14(08)**.

[15] Erin K. Lipp, Anwar Huq, and Rita R. Colwell. (2002). Effects of Global Climate on Infectious Disease: the Cholera Model, *Clin Microbiol Rev,* **15(4)**, 757–770.

[16] Fauci B., Isselbacher, Kasper H., and Wilson M,. (1998). Pinciples of internal medicine, *Journal of Biological Dynamics,* **02(07)**, 020291-5.

[17] Guckenheimer, J., Holmes, P. (1983). Nonlinear Oscillations,Dynamical Systems and Bifurcations of Vector Fields, *Springer, Berlin.*

[18] Global task force on cholera control. (2004). Cholera outbreak: assesing the outbreak response and improving preparedness, *WHO,* 42-43.

[19] Global task force on cholera control. (2022). Assesing the outbreak response and improving preparedness.

[20] G. Magombedze, N. M. Ferguson, and A. C. Ghani. (2018). A trade-off between dry season survival longevity and wet season high net reproduction can explain the persistence of anopheles mosquitoes, *Parasites Vectors,* **11(1)**.

[21] Helikumi, Mlyashimbi, Lolika, Paride. (2022). A note on fractional-order model for cholera disease transmission with control strategies. emphCommunications in Mathematical Biology and Neuroscience

[22] H. Guo, M. Y. Li, and Z. Shuai. (2006). Global stability of the endemic equilibrium of multigroup SIR epidemic models, Canad. Appl. Math. Quart.**14**, 259–284

[23] H. Guo, M. Y. Li, and Z. Shuai. (2012). Global dynamics of a general class of multistage models for infectious diseases, *SIAM J. Appl. Math.,* **72**, 261–279

[24] Igor Podlubny. (1998). Fractional differential equations: an introduction to fractional derivatives, fractional differential equations, to methods of their solution and some of their applications. *Elsevier.*

[25] J. P. LaSalle, (1976). The Stability of Dynamical Systems, *Regional Conf. Ser. Appl. Math., SIAM,Philadelphia.*

[26] Kelly G., (2006). Body temperature variability (Part 1): A review of the history of body temperature and its variability due to site selection, biological rhythms, fitness, and aging. *Altern Med Rev*,**11**, 278–93.

[27] Kelly G.,(2007). Body temperature variability (Part 2): Masking influences of body temperature variability and a review of body temperature variability in disease. *Altern Med Rev*, **12**, 49–62.

[28] Liu *et al*. (2008). SVIR epidemic models with vaccination strategies, *Biol* **253(1)**, 1-11.

[29] Mackowiak PA, Wasserman SS, Levine MM., (1992). A critical appraisal of 98.6 degrees F, the upper limit of the normal body temperature, and other legacies of Carl Reinhold August Wunderlich. JAMA, **268**, 1578–80.

[30] Md Arquam *et al*. (2019). Integrating Environmental Temperature Conditions into the SIR Model for Vector-Borne Diseases, *Complex Networks and Their Applications ,* **8(1)**, 412-424.

[31] Ngoteya FN., Gyekye YN. (2015). Sensitivity Analysis of parameters in a Competition Model, *Apple. Comput Math,* **4(5)**, 363-368.

[32] National library of medicine. (2015). *Int, J Eviron Res Public Health,* **(12)7**, 8034-8074.

[33] Salisu M. and Usman A. Danbaba. (2020). Mathematical Modelling of the effect of Temperature variability on malaria control strategies, *Math. Model. Nat. Phenom.***15(65)**

[34] Safieh, D. Rebwar, M. H. Hamed, M. A. H. Saeed , J. Forough. (2020). Investigation of water quality in wet and dry seasons under climate change, *Ukrainian Journal of Ecology.***10(5)**, 94-104.

[35] Sani Fakai Abubakar and Mohammed Olarenwaju Ibrahim. (2022). Caputo Sense Fractional Order Derivative Model of Cholera, *American Journal of Mathematical and Computer Modelling.* **7(2)**, 31-36.

[36] Saif Ullah, Muhammad Altaf Khan, and Muhammad Farooq. (2018). A fractional model for the dynamics of tb virus. Chaos, Solitons Fractals, 116:63–71.

[37] "Virus-Cell interaction and Viral Antimetabolies", *Shugar Academic Press, New York*, (1972).

[38] Van den D.P and Watmough J. (2002). Reproduction number and subthreshold endemic equilibria for compartmental models of disease transmission, *Math.Biosci.,* **180**, 29-48.

[39] World Health Organization. (2017), Cholera vaccines, *WHO position paper,* **92(34)**, 477-500.

[40] World Health Organization. (2023). Global Cholera Statistics for 2023. Web page. Available at: http://www.who.org.

[41] Wang J and Modnak C. (2011). Modelling cholera dynamics with controls, *Canadian Applied Mathematics Quarterly*, **19(3)**, 256-272.

[42] World Health Organization. (2022). *www.who.int/news-room/fact-sheets/detail/cholera?gclid*

[43] Wunderlich CR. (1968). Das Verhalten der Eigenwaerme in Krankheiten, Leipzig: *Verlag Von Otto Wigand.*

[44] X. Wang and J. Wang. (2017). Disease dynamics in a coupled cholera model linking within-host and between-host interactions, *J. Biol. Dyn.,***11(1)**, 238–262.

[45] X. Wang and J. Wang,(2017). Modeling the within-host dynamics of cholera: bacterial-viral interaction, *J. Biol. Dyn.,* **11(2)**, 484–501.

[46] Xueying W, Daozhou G and Wang J. (2015). Influence of human behavoir on cholera dynamics, *Mathematical Biosciences,***267**, 41-52.

[47] Xueying Wang and Jin Wang. (2017). Modeling the within-host dynamics of cholera bacterial–viral interaction, *Journal of Biological Dynamics,* **11**, 484-501

[48] Xueying Wang and Jin Wang. (2016). Disease dynamics in a coupled cholera model linking within-host and between-host interactions, *J. Math. Biol.* **26**, 445–492.